

INTERNSHIP CHEMICAL ENGINEERING

Techno-economic Evaluation of Potential Algae Refinement Plant

Internship Chemical Engineering
Groningen Seaports & Omega Green
Rijksuniversiteit Groningen, the Netherlands

Author:

J.R.J. BEUVING | S2536978

First Assessor:

PROF. DR. G.J.W. EUVERINK | UNIVERSITY OF GRONINGEN

Second Assessor:

PROF. DR. K. VAN DER VOORT MAARSCHALK | UNIVERSITY OF GRONINGEN

Company Supervisors:

M. SCHOONDORP | OMEGA GREEN
E. VAN DEN DOOL | GRONINGEN SEAPORTS
M. ZWERVER | GRONINGEN SEAPORTS

October 21, 2020

Abstract

Microalgae show an enormous potential as a feedstock for numerous bioproducts. The ability of algae to convert CO₂ into useful products increases the sustainability of the industrial region. *Chlorella vulgaris*, one of the limited microalgae approved for human consumption, shows promise to be used as a sustainable protein substitute due to its high protein content. In the current work a techno-economic evaluation is performed on the production of *Chlorella vulgaris* on a 40 hectare scale and the mild extraction of a carbohydrate rich fraction and a functional protein rich fraction through acid precipitation. The protein concentration of the main product, the protein rich fraction, was 63%. The economic evaluation of two refinement scenarios, immediate refinement and the introduction of a drying step, resulted in a maximum ROI of 37% over 30 years.

Contents

1	List of Abbreviations	3
2	Introduction	4
3	Biochemical Composition <i>Chlorella vulgaris</i>	5
3.1	General composition	5
3.2	Further specification of content	6
3.3	Physical and Chemical properties of Components	7
4	Algae Production Process	10
4.1	Photo Bio Reactor	11
4.2	VIBRO Ultrafiltration	12
4.3	Spray cooler	13
5	Downstream processing	14
5.1	Homogenization	15
5.2	Buffer capacity of proteins	17
5.3	Centrifugation	17
5.4	VIBRO-3	19
5.5	Spray dryers	19
6	Economic evaluation	20
6.1	Economic evaluation of algae production	21
6.2	Economic evaluation of the downstream processing	22
7	Discussion	25
8	Conclusion	26
A	Appendix A: Algae Production economic evaluation	34
B	Appendix B: Algae Refinery S1 economic evaluation	36
C	Appendix C: Algae Refinery S2 economic evaluation	38
D	Appendix D: Solar drying techniques	42

1 List of Abbreviations

CW	-	Cooling Water
DHA	-	Docosahexaenoic Acid
EPA	-	Eicosapentaenoic Acid
HPH	-	High Pressure Homogenizers
ITSD	-	Indirect Type Solar Dryers
LDPE	-	Light Density Polyethylene
LHC	-	Light Harvesting Complex
MFA	-	Monounsaturated Fatty Acid
MGDG	-	Monogalactosyldiaclycerol
PBR	-	Photobioreactor
PG	-	Phosphatidylglycerol
PL	-	Polar Lipids
PUFA	-	Polyunsaturated Fatty Acid
ROI	-	Return On Investment
SFA	-	Saturated Fatty Acid
UF	-	Ultrafiltration

2 Introduction

Groningen Seaports is the port authority and the commercial developer of the ports of Delfzijl and the Eemshaven and the surrounding industrial region. As the port authority, they take care of all the maritime logistical services within the ports. By attracting new companies and supporting already settled companies, Groningen Seaports takes an active role in the development of the industrial region surrounding the ports [1].

Omega Green is one of the companies settled in the Eemshaven which actively cooperates with Groningen Seaports in order to further develop themselves. Omega Green has developed a new production method for algae cultivation, consisting of low cost, modular, recyclable bioreactors which enables upscaling and affordable algae production [2]. Due to their high protein, fatty acids, polysaccharides and pigment content, algae accumulate many biochemicals with applications in health, cosmetics, pharmaceuticals, biofuels, food and feed. Compared to most of the current sources of these biochemicals, algae are expected to represent a green alternative, offering several environmental benefits [3, 4].

The ability of the system to convert CO₂ into useful product increases the sustainability of the industrial region, especially since the system is able to grow algae on direct or indirect flue gasses [4, 5]. Furthermore, algae can be grown on land unsuitable for agricultural use and on residual water streams or seawater with a higher areal productivity compared to other crops [5]. These synergistic advantages of algae growth and the process of Omega Green with other potential companies falls within the strategy of Groningen Seaports, attracting and developing companies working on waste streams and reducing the environmental impact of the industrial clusters [6].

Currently, Omega Green is investigating the possibility of up-scaling towards a 40 ha algae plant, which would result in an annual dry weight production of approximately 900 MT. The world market for dried *Spirulina* and *Chlorella*, the only algae species approved for human consumption in the European Union, are 12000 MT and 5000 MT respectively [7]. Entering the dried algae market with a potential market share of 7.5% and 18% for *Spirulina* and *Chlorella* respectively would most likely result in a significant reduction of product value, making whole algae production at such a scale unprofitable.

The introduction of downstream processing could make it possible to produce higher value products which target other markets. Omega Green is interested in the potential development of a downstream process which enables the recovery of a protein rich fraction suitable for usage as an ingredient in formulated foods. The protein enriched fraction could introduce beneficial structural and nutritional properties to formulated foods when the protein structure is maintained during extraction [8, 9]. Since only *Spirulina* and *Chlorella* are approved for human consumption in the EU, and growing *Spirulina* requires elevated temperatures incompatible with the climate in the north of the Netherlands, the evaluated algae during this research is *Chlorella vulgaris*, an extensively cultured microalgae [10].

During this research, a potential downstream process is developed which focuses on the recovery of a protein rich fraction suitable to be used in formulated foods for human consumption. Initially, the composition of *Chlorella vulgaris* is evaluated, followed by a model of the algae production and refinement process in order to determine the feasibility of such a process.

3 Biochemical Composition *Chlorella vulgaris*

The green microalgae *Chlorella vulgaris* is an important member in the aquatic food chain which shows promise as an alternative source of protein in food and feed applications [11]. *Chlorella vulgaris* can be grown photoautotrophic, heterotrophic, and mixotrophic and is being cultivated extensively around the world [10]. One of the advantages of using *Chlorella vulgaris* for the recovery of a protein enriched fraction is the nutritional value attributed to proteins of *Chlorella vulgaris*.

3.1 General composition

In order to design a downstream process which targets the isolation of a protein rich fraction, the composition of *Chlorella vulgaris* needs to be determined. An analysis by Omega Green on the composition of produced *Chlorella vulgaris* in their system has resulted in a composition with a protein, lipid, and ash content of 43.3%, 10.4%, and 13.7% respectively. This analysis lacks the carbohydrate and pigment content and needs in terms of its constituents. Furthermore, when looking at Table 1, it can be noticed that the lipid and ash content determined by Omega Green is not within the range found in literature. Nonetheless, the figures of the analysis of Omega Green are being used during this research.

To determine the carbohydrate content, the pigment content, and to further specify the individual components, literature using comparable growing conditions as the system of Omega Green, such as the photoautotrophic growing conditions, the light regimes, and medium composition, needs to be evaluated.

Tab. 1: Composition ranges of *Chlorella vulgaris* found in literature in DW%

Protein	Lipids	Carbohydrates	Ash	References
11-58	13-48	12-60	3-12	[10, 12, 13, 14, 15, 16, 17]

The effect of varying light regimes on the fatty acid, protein, and pigment content of *Chlorella vulgaris* was investigated by Seyfabadi et al. [10]. By altering the duration and the intensity of the lighting, variations in the protein, pigment, and fatty acid compositions were measured. The results depicted a positive relation in the amount of proteins and lipids with respect to light intensity. Furthermore, the chlorophyll content is inversely related to the lighting intensity whereas the β -carotene levels increased with increased lighting intensity [10, 11, 18].

The average lighting intensity experienced in the Netherlands is equal to $21 \text{ molm}^{-2}\text{d}^{-1}$ [19]. This is similar to the light intensity used in the cultivation of *Chlorella vulgaris* by Griffiths et al., at a Photo Flux Index of $21.6 \text{ molm}^{-2}\text{d}^{-1}$ [20], which focuses on the influence of nitrogen concentrations on the compositions of *Chlorella vulgaris*. Their results depict an inverted relation between the lipid content and nitrate concentration in the medium, whereas the pigment and protein content increased with elevated nitrate concentration [20]. At a nitrogen concentration of 750 mgL^{-1} , the nitrogen concentration used by Omega Green, the carbohydrate content equals approximately 29 DW% whereas the pigment content is approximately 3-4% [20].

The pigment content of 3-4% is similar to other literature, which led to the assumption of a pigment content for *Chlorella vulgaris* of 4% [11, 15, 20, 21]. The remaining content is assumed to be equal to the carbohydrate content, which with the set lipid, protein, pigment and ash content, equals 28.6 %, close to the previously reported 29% [20]. This results in the final assumed composition for lipids, proteins, carbohydrates, pigments, and ash of 10.4%, 43.3%, 28.6%, 4.0%, and 13.7% respectively.

3.2 Further specification of content

To further specify the composition of *Chlorella vulgaris*, the lipid profile needs to be determined. The composition is simplified by assuming that only polar lipids, triacylglycerides, waxes, and sterols are present. The lipid profile is, just as the total lipid concentration, affected by the growing conditions, such as the used light regimes and the composition of the medium [15, 22, 23]. The works of Chia et al. researches the effect of nitrogen and phosphate concentration at a lighting intensity of $13 \text{ molm}^{-2}\text{d}^{-1}$ [22, 23]. By taking the average composition of the lipids in both works from the control conditions, without depletion of either nitrogen and phosphate, the composition of polar lipids, triacylglycerides, sterols, and waxes are determined at 93%, 1%, 2%, and 4% of the total lipid content respectively [22, 23]. Furthermore, the fatty acid profile of the polar lipids and triacylglycerides after saponification are retrieved from the average between the works of Tokuşoglu et al. and Chia et al., with a saturated fatty acid (SFA), monounsaturated fatty acid (MFA) and polyunsaturated fatty acid (PUFA) composition of 20%, 26%, and 54% of the polar lipids and triacylglycerides content respectively [15, 22].

Besides using the works of Tokuşoglu et al. and Chia et al. in the determination of the fatty acid profile in terms of SFA, MFA and PUFA, the average omega 3 content (42% total fatty acids) of both works were used [15, 22]. The research of Tokuşoglu et al. was used to estimate the DPA and EPA content of the PUFA, which were scaled according to the previously determined total ω -3 content [15]. Both the methods of des

Tab. 2: Fatty acid distribution of polar lipids and triglycerides in DW% in terms of SFA MFA and PUFA (a), and ω -3 content and composition of PUFA in DW% of algae (b)

<i>a</i>	DW%	<i>b</i>	DW%
SFA	2.0%	ω -3	4.1%
MFA	2.5%	DHA	2.9%
PUFA	5.3%	EPA	0.4%

Pigments are generally divided into two groups, the carotenoids, such as lutein, β -carotone, and zeaxanthin, and the chlorophylls, which consists of chlorophyll- α and chlorophyll- β . The composition of the pigments differs widely between different studies due to differences in the used extraction methods and algae growing conditions [24, 25, 26]. The carotenoids are mostly of interest due to their antioxidant behavior, with lutein being the main carotenoid found in *Chlorella vulgaris*. Lutein content in *Chlorella vulgaris* in literature focused on the retrieval of pigments show concentrations ranges of 3.86 and 9.82 mg/g DW, with an average of 6.26 mg/g DW [27, 28, 29, 30, 31]. Chlorophyll content in the same and similar literature differs between 15.4 and 45.25 mg/g DW, averaging at 30 mg/g DW [24, 28, 31, 32]. These averages translate in a DW% of 0.63 and 3.0 DW% for lutein and chlorophylls respectively. The residual pigments content were ascribed to the other cartenoids present in *Chlorella vulgaris* besides lutein.

The carbohydrates can be divided into two groups, the polysaccharides and the monosaccharides. Ferreira et al. used a holistic approach to separate the carbohydrates from *Chlorella vulgaris*, in which several separation steps were performed of which each fractions carbohydrate, lipid and protein content was measured [33]. Their results show that the majority of the carbohydrates consist of glucose units with 74 mol %, followed by galactose and rhamnose with 10.3 mol% and 4 mol% respectively. The remainder of the sugars present in *Chlorella vulgaris* are made up of fraction of mannose, xylose, arabinose and fucose [33].

The majority (76.6%) of these sugars were present in the form of starches, with an amylose/ amylopectin ratio of 3:7, similar to other studies concerning the characterization of starch derived from *Chlorella vulgaris* [33, 34]. The remaining carbohydrates were considered to be other mono and polysaccharides for which no differentiation was made. This results in an assumed composition of the carbohydrates of 22 DW% and 6.6 DW% for polysaccharides and monosaccharides respectively.

The nutritional value of proteins found in algae is determined by the content, proportion and availability of the amino acids. *Chlorella vulgaris* has a high essential amino acid profile, with a concentration of 38%. The major amino acids are alanine and glutamic acid with 10.7% and 10.3% respectively [35].

This results in the final assumed composition of *Chlorella vulgaris*, which is depicted in Table 3.

Tab. 3: Assumed final composition of *Chlorella vulgaris* in DW%

Component	DW%
Lipids	10.4%
<i>Glyco-Phospholipids</i>	9.7%
<i>Triglycerides</i>	0.1%
<i>Sterols</i>	0.2%
<i>Waxes</i>	0.4%
Proteins	43.3%
Carbohydrates	28.6%
<i>Monosaccharides</i>	6.6%
<i>Polysaccharides</i>	22.0%
Pigments	4.0%
<i>Chlorophylls</i>	3.0%
<i>Lutein</i>	0.63%
<i>Other carotenoids</i>	0.37%
Ashes	13.7%

3.3 Physical and Chemical properties of Components

In order to design the process the physical and chemical properties of the components need to be investigated. To simplify the process design, only the major consistent is assumed to make up each component.

3.3.1 Lipids

The main type of lipids found in *Chlorella vulgaris* are glyco- and phospholipids, both present in the membrane of the algae [22, 23]. Glycolipids are complexes consisting of lipids and a carbohydrate, attached by a glycosidic bond [36]. The main type of glycolipid found in *Chlorella vulgaris* is monogalactosyldiaclyglycerol (MGDG). Phospholipids consists of two fatty acids and a phosphate ester, connected by an alcohol. Phosphatidylglycerol (PG) is the main type of phospholipid found in *Chlorella vulgaris*. Both MGDG and PG are predominantly composed of 16- and 18-carbon fatty acid groups which are often unsaturated, as shown by the high PUFA content depicted in Table 2 [36, 37]. Both MGDG and PG have a M_w of approximately 0.75 kDa, depending on the composition of the attached fatty acid chains. Their molecular diameters were estimated with the group contribution method of van Krevelen to determine the molar volume with a non-globular factor of 2.0, resulting in 1.4 nm [38]. Furthermore, the density of 855 kg/m³ was obtained from

the calculated molar volume.

Due to the polarity of MGDG and PG, the lipids are likely to form micelles if the critical micelle concentration is reached. If the concentration surpasses the critical micelle concentration, it is assumed that spherical micelles are formed. A micelle diameter of 4.11 nm was derived from the molecular volume with an assumed aggregation number of 100 [39]. The effect of salinity on the micellization of PG due to its ionic nature is disregarded to limit the complexity.

Oils rich in unsaturated bonds, such the lipid fraction of *Chlorella vulgaris*, are prone to lipid oxidation which limits the utilization in processed foods and in nutritional supplements [40]. Lipid oxidation results in the formation of potential toxic compounds and undesirable flavors, reducing the nutritional quality of the extract [41]. Increasing the oxidation stability is necessary to prolong the shelf life of PUFA extracts, which can be achieved by the addition of a combination of antioxidants [42]. Antioxidants have the ability to delay or prevent the oxidation of an oxidizable substrate when present in low concentrations by removing metal ions, the scavenging of radicals, and by the quenching of singlet oxygen [42].

3.3.2 Proteins

More than 200 species of proteins are present in *Chlorella vulgaris*, distributed in several classes [35]. The major protein classes found in *Chlorella vulgaris* are ribulose-1,5-bisphosphate carboxylase/oxygenase, commonly referred to as RuBisCO, and chlorophyll-containing light-harvesting complexes (LHC) [43]. In algae, mainly RuBisCO in the so called form I is found, consisting of 8 large and 8 smaller sub units. The M_W of the large and small sub-units differ, ranging between 50-55 kDa and 10-17 kDa respectively. The combined RuBisCO complex has a M_W of approximately 540 kDa. The M_W of the LHC range from 20-32 kDa [9].

In the work of Ursu et al., the SDS-Page analysis and SEC chromatogram of functional protein fractions recovered from *Chlorella vulgaris* after filtration, show the presence of proteins with a M_W of approximately 30 kDa and 60 kDa, similar to the the LHC and small RuBisCO sub units, and the large RuBisCO sub units respectively [35]. However, the majority of the detected proteins are present as macromolecules with a high M_W , above 670 kDa [35]. These macromolecules were identified as complex soluble aggregates of proteins and the LHC, and amount to approximately 80% of the total protein content [31, 35]. Solely attributing the high M_W macromolecules to aggregates of proteins and the LHC disregards the possibility of the presence of protein originating from the structural protein in the cell membrane, which could be soluble due to the used high pressure cell lysis [44, 35]. The molecular diameter of the protein aggregates were estimated according to the method of Erickson, resulting in 19.8 nm if a M_W of 1000 kDa is assumed with a spherical correction factor of 3 [45].

The solubility of these proteins is drastically dependent on the acidity of the solution. Two ranges of isoelectrical points were identified by Ursu et al., a minor fraction is insoluble at pH values of 6-8, whereas the majority of the proteins have their isoelectrical points at pH values of 4-5 [35]. This is similar to other green algae, where the majority of the protein fractions precipitate at pH values of 4-5 at varying ionic strengths [9]. The precipitation will result in increased protein aggregates, forming larger particles which can be separated through centrifugation. The assumed size of the protein aggregates is based on studies involving pure soybean protein precipitation, which mention a typical precipitated protein aggregate size of 1-50 μm [46, 47]. Since the algal protein is present in mixture during precipitation, an aggregate size of 1 μm is assumed.

Furthermore, to recover a fraction containing a high degree of functional proteins, denaturation must

be limited. Denaturation is the loss of secondary and tertiary structures of proteins, which is the result of exposure to external stress, such as heat, acidic or basic conditions, radiation, and organic solvents [35, 48, 49]. Long term exposure to temperatures above 30 °C will result in denaturation and loss of secondary structure in beet root protein [8]. It is assumed that the algal proteins react in a similar manner. Emulsifying capabilities of proteins decrease slightly compared to mild extractions when the extraction is performed at a pH of 12 [35]. Contact with organic solvents should be avoided, since solvents can disrupt the structure through two different mechanisms. The first mechanism can be attributed to the disruption of hydrogen bonds within the protein if the protein is soluble in the solvent [48, 50]. The second mechanism takes place at the water-solvent interface. Hydrophobic patches on the protein surface will be attracted towards the solvent interface, leading to unfolding [48].

3.3.3 Carbohydrates, ash and pigments

As previously mentioned, two types of carbohydrates are present in *Chlorella vulgaris*, monosaccharides and polysaccharides. During this research, the assumption is made that all polysaccharides are present as starches, ignoring polysaccharides with other origins, such as the cellulose fractions found in the algal cell wall [51]. The starch granules, with an amylose content of 30% and an amylopectin content of 70%, have an average M_w of 6.35×10^8 [33, 52]. Based on the method of Erickson et al., this translates to a particle diameter of 1.1 μm [45]. The solubility of native starches with similar amylose content in 1 M NaOH at 25 °C after 15 h is equal to 7.6 g/L [53]. The only assumed constituent for the monosaccharides is glucose. The M_w of glucose equals 0.18 kDa, with molecular size of approximately 1 nm, and a solubility at room temperature of 909 g/L. The ash content consists of several minerals, where the main constituents are sodium and calcium particles [54]. The ash particles are assumed to be completely water soluble, similar to the glucose particles. From the two main pigments found in *Chlorella vulgaris*, chlorophyll has the largest share with 75%. The M_w equals 0.895 kDa, which would result in a similar order of size as MGDG and PG, below 1 nm. However, fractioning of *Chlorella vulgaris* has shown that the chlorophyll is bounded to the LHC due to the vivid green color of protein fraction [31, 35]. Removal of pigments from the protein fraction will require the usage of organic solvents or supercritical CO_2 , which will result in denaturation of the protein [33, 55, 56].

Tab. 4: Physical Properties of components

Component	Specific heat (kJ/kgK)	Density (kg/m ³)	Mw (kDa)	Size (nm)
Protein	1.47	1125	1000	19.2
Protein Precipitates	1.47	1125	52083	1000
Starch		1500	6.35E+08	1300
Glucose	0.115	1500	0.18	1.00
Polar Lipids	2.3	855	0.75	1.41
Micelles	2.3		75	4.11
Biomass	1.58	1050		5000
Water	4.18	997		0.27
Ash	0.73			
Pigments	1.47		0.895	0.65

4 Algae Production Process

Omega Green has developed an efficient and sustainable growing system aimed at a low price production of the algae. The process consists of low density polyethylene (LDPE) bags which require no cleaning and, due to the closed and controlled nature of the production process, are suitable for food and feed production. This system is currently being developed further in the Eemshaven, where a standard unit of 2500 m² is present. In Morocco, a 1 ha production system is being used which utilizes flue gasses from a concrete production plant [2].

During this research, SuperPro Designer is used to obtain a model of the upscaled production facility and the refinery process. An overview of the system is given in Figure 1, which consists of the algae production and the dewatering steps.

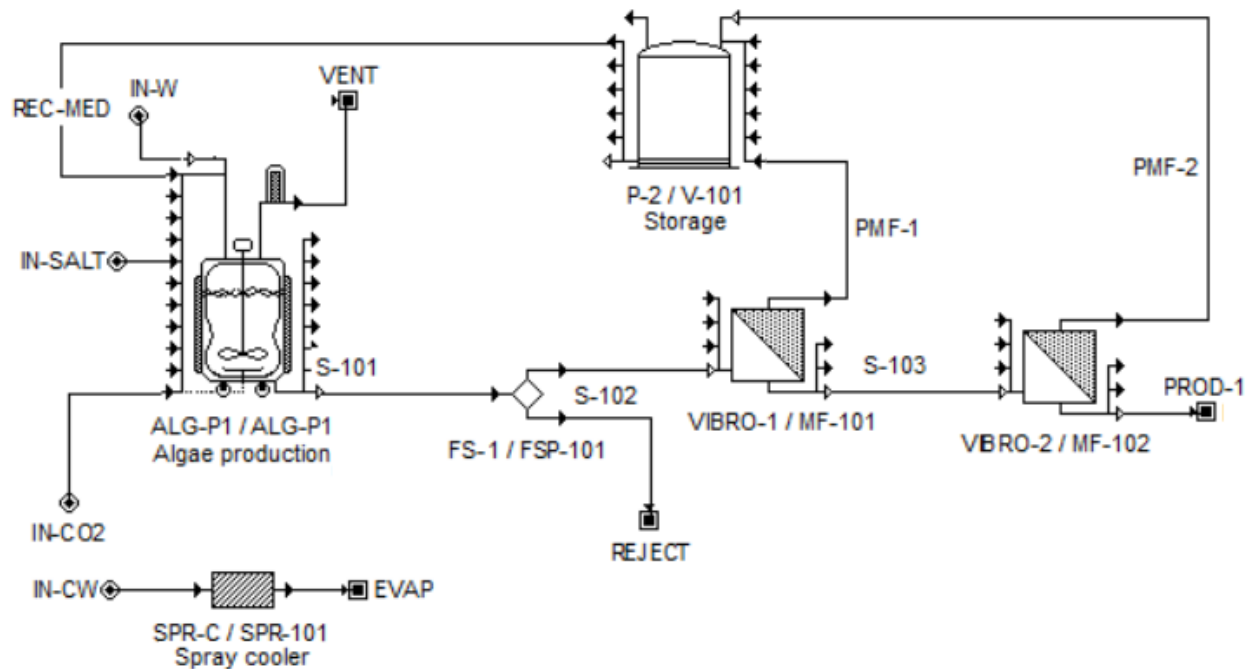


Fig. 1: Model of Omega Green algae production system with dewatering based on VIBRO-I technology

The process consists of a disposable Photo Bio Reactor (PBR), two Ultra Filtration (UF) units, a storage for the permeate and an additional spray cooler which cools the algae. Initially, the reactor is loaded with the growing medium, consisting of recovered medium from the previous batch and new medium. This is followed by the fermentation step, which is fed CO₂ throughout the whole step. After fermentation, 30% of the reactor volume is harvested. 10% of the harvested volume is rejected, while the remainder passes through the two UF filtration units to concentrate the algae. The permeate of the filtration units is recovered and recycled into the next batch.

A 1 ha production field is expected to produce 25 MT of algae annually. However, the dependency of the algal growth rate on the available lighting will result in large differences in material consumption and biomass production for each month. Nick Terra (intern Omega Green) has produced a monthly mass balance based on the lighting regimes and temperature dependencies of algae production retrieved from Schipperus et al. and Spruijt et al. [57, 58]. In this mass balance, the production of 25 ton per ha is distributed over each production month based on the available lighting, whereas both the lighting and temperature distribution are used to evaluate the required amount of water

to compensate for evaporation. The production season starts in March and finishes at the end of October, translating to a 35 week season. The 30% harvesting volume is kept constant, while the obtained biomass concentration varies during the season. By decreasing the harvesting frequency at low production, thus extending the duration of fermentation, the harvesting concentration is kept above 0.4 g/L for the total biomass. The consequence of changing the harvesting frequency is a variable batch time. The batch time equal 24 h, 29.5 h, and 56 h during maximal, average and minimal production at the chosen harvesting frequencies. The production rates at maximum, average and minimal production equal 189, 125 and 54 kg biomass per batch respectively. The total amount of batches per year equals 7975, resulting in the production of 1000 MT of biomass annually for the 40 ha production site when the average production is assumed.

4.1 Photo Bio Reactor

The disposable PBR has been modelled to contain 4 disposable LDPE bags of 120 m³ each, resulting in a reactor volume of 480 m³. During production, the batch volume equals 430 m³, representing the volume of a 1 ha production facility of Omega Green. By staggering an additional 39 reactors, the aimed facility size of 40 is reached. Purchase costs are set at €9000 for each hectare with a price of € 7200 for each disposable LDPE bag. Prices are derived from economic evaluations performed by Omega Green, considering a 20% cost reduction for the production of the LDPE bags due to upscaled production.

The process of the PBR consists of three raw material inputs, where water, medium salts and carbon dioxide enter the reactor through IN-W, IN-SALT and IN-CO2 respectively. The medium is composed of several salts to provide the required nutrients for the algae, which are depicted in Table 5. This is a simplification of the mixture used by Omega Green for the production freshwater algae at a concentration of 1.1 g/L (total salts/water), which besides the salts depicted in Table 5 contains an iron and a stimulus solution. The consumption of these mixtures are neglected to simplify the simulation. Furthermore, a small alteration was made in the ratio of KH₂PO₄, which is reduced according to its consumption to prevent accumulation.

Tab. 5: Assumed medium composition for freshwater and consumption during an average batch

Component	wt%	[C] (g/L)	m (kg/batch)
KNO ₃	76.5%	0.841	78.1
KH ₂ PO ₄	11.2%	0.123	11.4
MgSO ₄	7.5%	0.082	7.6
Ca(NO ₃) ₂	2.4%	0.027	2.5
NaCl	2.4%	0.027	2.5
Total			102.1

The conversion of input materials towards biomass is based on a stoichiometric model of the fermentation reaction. The salt consumption is based on the nitrogen and phosphate content of the algae. 1 kg of algae contains 76.5 g nitrogen and 17.6 g of phosphorus [15]. This translates to 0.529 kg KNO₃ and 0.017 kg Ca(NO₃)₂ per kg biomass for the nitrogen consumption, whereas 0.077 kg of KH₂PO₄ is sufficient to cover the phosphorus consumption. Furthermore, single ions are not considered during the simulation, converting all residual mass towards oxygen. The downside of this assumption is that ion accumulation cannot be identified using this model. The CO₂ consumption is based on the ratio 1.843:1 (CO₂:biomass)[59]. With pH controlled addition of CO₂, efficiencies of 90% (CO₂ added vs CO₂ converted) have been achieved in closed systems [60]. In this model, an efficiency of 70% is assumed. However, CO₂ has been set as the rate limiting component in

the fermentation reaction which assumes a 100% efficiency. This has been compensated by only feeding 70% of the CO₂ through the reactor, while the excess of 30% is fed through the spray cooler to obtain the desired consumption. The stoichiometry of the fermentation reaction is depicted in Table 6. The energy consumption of the reactors is set at 5.625 kWh, derived from the energy balance provided by Omega Green.

Tab. 6: Stoichiometry of the fermentation reaction

Reactants	(kg)	Products	(kg)
CO2	184.3	Biomass	100.0
KNO3	52.9	Oxygen	153.4
KH2PO4	7.7		
MgSO4	5.2		
Ca(NO3)2	1.7		
NaCl	1.7		
Total	253.4		253.4

4.2 VIBRO Ultrafiltration

The filtration units are based on information retrieved from communication between Omega Green and SANI-membranes. The VIBRO-I is an industrial filtration solution which achieves high flux at low energy, delivering continuous low fouling filtration due to the introduction of vibration shear [61]. The filtration unit consists of modular 2.5 m² units, which can be stacked up to 60 m² for a single unit (3*20 m²). Membrane cut-offs are available for ultrafiltration and microfiltration.

The data used to model the VIBRO filtration units in SuperPro derived from communications between SANI-membrane and Omega Green are depicted in Table 7. It depicts three different setups and their characteristics. The permeation rates differ significantly, depending on the final concentration.

Tab. 7: Characteristics of SANI-membrane VIBRO filtration units

Concentrations		Max factor	Maximal area	MF/UF	Permeation rate
initial (g/L)	final (g/L)	(final/initial)	(m²)		(L/hm²)
0.3	7	10	60	MF	63.3
3	24	8	20	UF	17.5
3	180	60	27.5	UF	14.1

The desired biomass concentration in the PROD-1 stream is set according to the homogenization method, discussed in section 5.1, which equals 24 g/L. To achieve the desired concentration, a combination of the MF unit and the UF with a permeation rate of 17.5 L/hm² is needed. Due to the varying harvesting concentrations and batch times throughout the year, the filtration setup needs to be changed accordingly. The fermentation, filtration and charging times are set at 90%, 5% and 5% of the total batch time respectively. The MF unit is assumed to concentrate the feed to either the maximal final concentration, or towards the maximal final/initial concentration factor. The UF unit concentrates the biomass towards the desired 24 g/L. The maximal number of MF and UF units are needed during maximal production. In total, 44 MF (60 m²) and 92 UF (20 m²) units are needed to concentrate the product flow. The large difference between the required units compared to the average and minimal production result in a significant fraction of units which are not utilized besides during peak performance. Energy consumption was set at 0.08 kW/m²

membrane area, 40% of the standard energy consumption of SuperPro based on energy reduction claims of SANI-membranes, which argue a 50-80% energy reduction is possible with the VIBRO-I technology [62].

Tab. 8: Modelled conditions of VIBRO-I filtration units at varying production rates

Production	Biomass (kg/batch)	t_{filt} (min)	S-102 Biomass	S-103 concentration	PROD-1 (g/L)	VIBRO-1 Units/parallel setups	VIBRO-2
Min	48.52	336	0.43	4.30	24.00	5/4	8/4
Average	113.3	176.96	1.00	7.00	24.00	9/4	14/4
Max	170.72	130.9	1.51	7.00	24.00	11/4	23/4

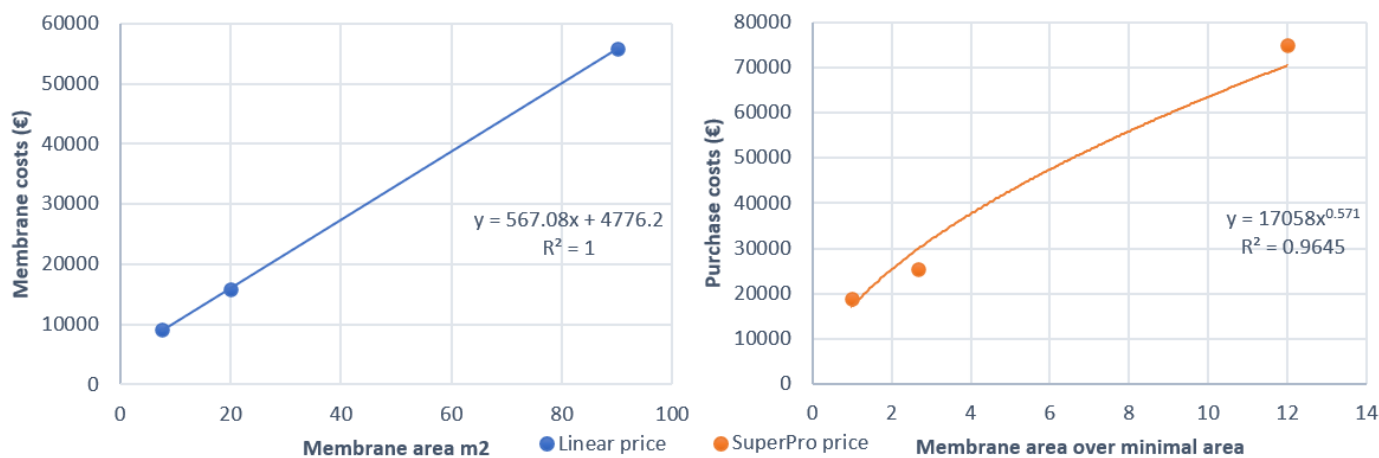


Fig. 2: VIBRO-I costs model assumptions

Finally, purchase costs and membrane consumption costs were determined by using three price quotations. By subtracting the control unit costs from the quotations, a linear trend found between the quotations as depicted in Figure 2. This has resulted in a membrane price of €567.08 per m^2 . Furthermore, SuperPro enables the usage of a user purchase costs model in the form $PC = C_0(Q/Q_0)^a$, where PC equals the purchase costs, C_0 the base costs, Q equals the membrane area in m^2 , Q_0 the minimal area of 7.5 m^2 and a as the exponent. By plotting the complete quotations over the membrane area divided by the minimal area, the values for C_0 and a were determined as 17058 and 0.571 respectively, as depicted in Figure 2.

4.3 Spray cooler

A closed production system such as the PBR developed by Omega Green has the advantage that heat and evaporative losses are minimized during cooler periods. However, overheating is possible during the warm periods, resulting in temperatures exceeding the tolerated temperature of the algae [3]. To prevent overheating from occurring, Omega Green has developed a spray cooler which activates when medium temperatures exceed the upper limit for the algae. The water consumption is modelled based on the temperature and wind conditions, resulting in an average water consumption of 17.96 m^3 per batch. The energy consumption, based on the energy balance of Omega Green, was set at 0.625 kW.

5 Downstream processing

Omega Green wants to develop a process in which a functional, protein rich fraction is separated from a carbohydrate fraction. Such a refinement of biomass is already applied by Rubisco Foods and Royal Cosun, who have successfully developed extraction processes of these fractions for onion toppings, duckweed, and sugarbeet roots [8, 56, 63]. Initially, only the protein rich fraction was considered to be the main product as a food supplement by Rubisco Foods, with values ranging from 10-25 € per kg. However, the high fiber and polysaccharide fraction has shown to have beneficial properties as an ingredient in foods, elevating taste by introducing a umami flavour and emulsifying capabilities of commercial sauces [56, 63].

Their processes are able to extract a high content native protein fraction through acid precipitation, based on the isoelectric point of the proteins. Each of their patented process designs consists of five basic steps, a homogenization step to disrupt the cell walls and release their constituents, elevation of the pH to dissolve the proteins, separation of a high fiber and polysaccharide fraction through filtration or centrifugation, followed by protein precipitation by acid introduction, and again separation through filtration or centrifugation. The exact pH at which dissolution and precipitation occurs differs for each patent and are based on the protein solubility curves. During this research, the protein solubility curves of Teuling et al. are used which depict the solubility of proteins from several green microalgae [9]. These conditions are comparable to the conditions used with the onion toppings and duckweed processes, with a pH of 8.3 and 4.2 during dissolving and precipitation [9, 56, 63].

The mild conditions of the process results in the extraction of proteins which maintain their tertiary structure, enabling their application in the foods industry due to their functional properties, such as good solubility, emulsifying capabilities, and gelling behavior [9]. It must be taken into account that during this research native and functional proteins are defined as proteins which maintain these functional properties, not as isolated proteins with enzymatic activities. The benefit of this type of process is its relative simplicity of the equipment, while the value of the product and the size of the potential market is increased.

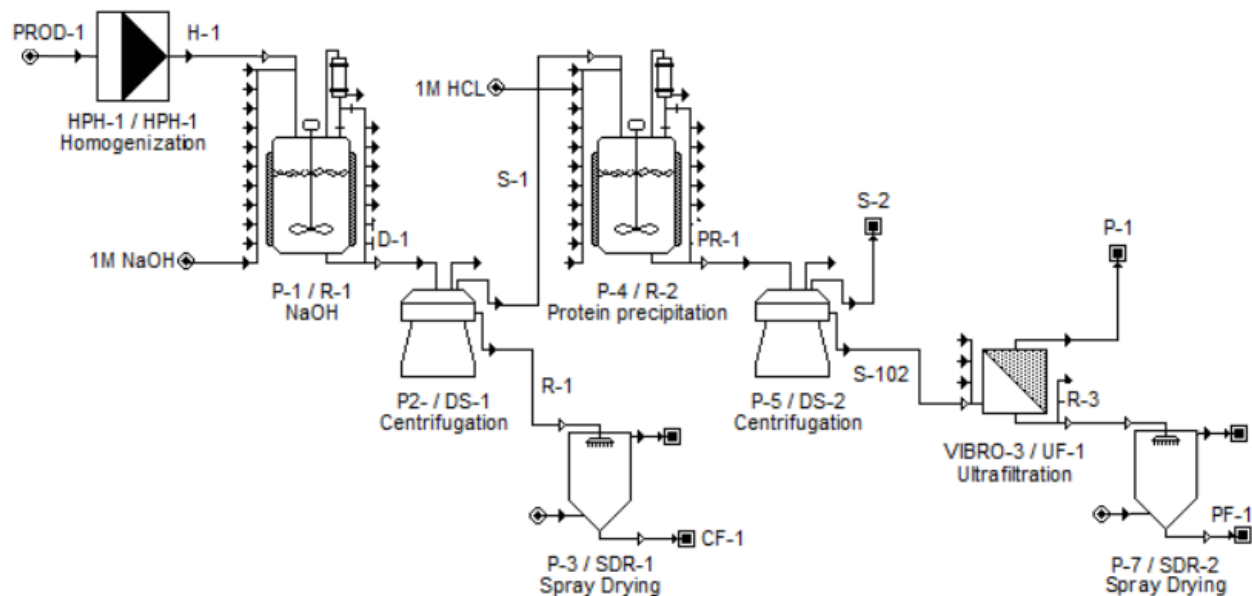


Fig. 3: Process design of refinery

The five basic steps are depicted in Figure 3, which starts with the algae from the production process, PROD-1, which undergoes the homogenization step. The pH is raised towards 8.3 in CISTR R-1 by the addition of NaOH. The residence time equals 1 h to dissolve the maximal amount of protein, similar to the process for sugar beet roots [8]. The first separation step is performed by the stacked disk centrifuge DS-1, separating the undissolved high polysaccharide fraction from the dissolved proteins. This fraction is spray dried in SDR-1, to obtain the carbohydrate enriched fraction in CF-1, the side product.

The liquid containing the dissolved proteins from DS-1 are transported towards CISTR R-2 through S-1, where the pH is decreased with HCl towards 4.2 to precipitate the proteins. The residence time of R-2 equals 1 h to ensure maximum precipitation. The second separation step is performed in the second stacked disk centrifuge DS-2, where the precipitated proteins are removed. The enriched protein fraction is further dewatered in the UF-1, desalinating the fraction before being dried in spray drier SDR-2, resulting in the enriched fraction PF-1. The characteristics and the assumptions made for each of the process steps are explained in the following sections.

5.1 Homogenization

To obtain the protein rich fraction of *Chlorella vulgaris*, a cell disruption or lysis step is needed to release the components. The cell wall of *Chlorella vulgaris* is predominantly composed of saccharides and cellulose, resulting in a thick cell wall which hinders the release of the desired components [51, 64]. Cell lysis methods are known to be significant operational costs due to their high energy and chemical consumption, or the methods require expensive maintenance intensive equipment [65]. The disruption methods can be separated into mechanical and non-mechanical methods, where the non-mechanical methods can be further divided into chemical, physical and biological methods. Mechanical methods, such as High Pressure Homogenizers (HPH) and bead milling, are highly effective in disrupting the cells and have been applied on an industrial scale. However, they require extensive cooling to limit the damaging effect of the generated heat [66]. The non-mechanical disruption methods have other disadvantages, such as a damaging effect on the proteins (thermal lysis, cavitation, detergent lysis), usage of expensive reagents (enzymatic lysis), and the duration of the process (chemical lysis) [66]. Due to the higher effectiveness of the mechanical methods and their application at a larger scale, the comparison between cell disruption methods during this research is limited to HPH and bead milling [66, 67].

HPH forces cells in media through an orifice valve using high pressure, subjecting the cells to high shear forces due to the compression of the cells at the entry of the orifice and the expansion of the cells during discharge [66]. The increase of pressure on the fluid will result in an increase in temperature. This is a beneficial effect when HPH is used for pasteurization, while being undesirable when functional proteins need to be extracted from algae [68]. When used to disrupt the cell wall of the algae, extensive cooling will be required to protect the desired constituents.

Several studies have used HPH to disrupt the cell walls of *Chlorella vulgaris* with the goal of obtaining functional proteins [31, 35, 69]. With a *Chlorella vulgaris* concentration of 24 g/L, Kulkarni et al. obtained a protein solubility of 75.6% with 3 passes at a pressure of 103.4 Mpa at neutral pH [31]. Ursu et al. obtained 98% and 67% protein solubility with 2 passes of a 13 g/L medium at 270 Mpa with a pH of 12 and 7 respectively [35]. In the work of Grossmann et al. 46% of the proteins in *Chlorella protothecoides* were solubilized in 6 passes at 150 MPa at a pH of 6.5 [69].

Bead milling uses glass, steel, or ceramic beads to agitate the cells, disrupting the cell walls during collision and releasing the intracellular components [66]. The effectiveness of the process is influenced by several parameters, such as the bead size and its material, cell concentration, and contact time.

Besides the HPH method, Kulkarni et al., used bead milling as a disruption method at 24 g/L with 0.5 mm glass beads, where a contact time of 900 seconds was sufficient to solubilize 75.6% of the protein at neutral pH [31]. Safi et al. performed bead milling at an increased *Chlorella vulgaris* concentration of 77 g/L, obtaining a 96% protein solubility [70]. Postma et al. investigated the energy consumption of bead milling on several types of microalgae [71]. On *Chlorella vulgaris* with a concentration of 60 g/L, a protein solubility of 36% was achieved using 0.4 mm beads with a contact time of 500 s [71].

To compare the disruption methods, both the bead milling and HPH were simulated in SuperPro designer based on the disruption of 126 kg biomass per hour. The results of the simulation are depicted in Table 9. Several assumptions were needed in order to compare the homogenization methods. The protein solubility of the studies performed at neutral pH was increased to compensate for the increase protein solubility at higher pH levels, with a factor of 1.11 obtained from Teuling et al. [9]. CAPEX costs were determined by the SuperPro cost model. The costs per kg solubilized protein were calculated using a depreciation period of 15 years, a kWh price of € 0.096, and a cooling water (CW) price of € 0.40 per m³. The results depicted in Table 9 show a major difference between the homogenization methods. HPH is mainly costly in energy and cooling water consumption, while the majority of the costs for bead milling is caused by the depreciation costs.

Since the functional proteins are targeted, all cost calculations are depicted per kg of solubilized protein to create a suitable comparison. HPH with a pressure of 103.4 Mpa and a concentration of 24 g/L is the most cost effective per kg of solubilized protein, with € 1.30 per kg of solubilized protein compared to € 1.40 per kg of solubilized protein for bead milling with a concentration of 77 g/L. This resulted in the decision to use HPH with a biomass concentration of 24 g/L as the method for cell disruption. The maximal throughput for HPH-1 equals 20 m³/h, the power to heat dissipation is set at 95% while the exit temperature is set to 30°C to limit the denaturation of the protein.

Tab. 9: Comparison of simulated bead milling and high pressure homogenization, with the protein solubility determined as the percentage of total protein solubilized (kgSP = kilogram solubilized protein).

Bead milling								
Bead size (mm)	Conc. (g/L)	Contact time (s)	Protein solubility (%)	E (kWh /kgSP)	CW (m3 /kgSP)	CAPEX	Costs (€/kgSP)	Ref
0.4	60	500	36%	10.2	1.6	€ 4,940,000	€ 3.71	[71]
0.5	24	900	84%	4.4	0.7	€ 11,856,000	€ 3.02	[31]
1.6	77	2400	96%	3.9	0.6	€ 4,940,000	€ 1.40	[70]

High Pressure Homogenization								
P (Mpa)	[Conc] (g/L)	Passes	Protein solubility (%)	E (kWh / kgSP)	CW (m3/kgSP)	CAPEX	Costs (€/kgSP)	Ref
270	13	2	75%	36.5	5.9	€ 196,000	€ 5.00	[35]
270	13	2	98%	27.8	4.5	€ 196,000	€ 3.80	[35]
103.4	24	3	84%	10.2	1.5	€ 101,000	€ 1.30	[31]
150	10	6	51%	115.8	19.0	€ 436,000	€ 16.00	[69]

During homogenization, it is assumed that 100% of the biomass is converted into its constituents

depicted in Table 10. The properties of each constituent is set according to the values present in Table 4.

Tab. 10: Homogenization of biomass into its constituents

Reactants	(kg)	Products	(kg)
Biomass	100.0	PL	10.4
		Protein	43.3
		Starch	22.0
		Glucose	6.6
		Pigments	4.0
		Ash	13.7
	100.0		100.0

5.2 Buffer capacity of proteins

Proteins have the ability to act as pH buffers due to the ionizable groups present on the polypeptide chains, such as the amino acids, terminal amino groups, and the terminal carboxylic acid groups [72]. In order to calculate the amount of NaOH and HCl needed to achieve the desired pH values of 8.3 and 4.2, an estimation of the buffer capacity for the proteins needs to be made.

In the work of Mennah-Govela et al., titration experiments have been performed on several mixtures of whey and egg protein [73]. The egg protein mixtures are used as comparison to the algae protein, due to a similar glutamic acid and aspartic acid content [35, 73]. The protein size has an effect on the buffer capacity, since amino acids can be hidden inside the protein structure [72]. The buffer capacity of proteins with small, medium and large particle sizes were evaluated at concentrations of 9.5, 13.3 and 17.2 wt%, whereas the protein concentration during both the addition of NaOH in R-1 and the HCl in R-2 is approximately 1 wt% of the total mixture. Since the exact sizes of the protein used in the work of Mennah-Govela et al. are unknown, the average buffer capacity is calculated from the extrapolated results towards the concentration of 1wt%, which equals $0.0155 \text{ mmol/pH kg}_{protein}$.

This value is used to determine the additional amount of NaOH and HCl needed besides the $1.99 \cdot 10^{-6} \text{ mol/L}$ NaOH to obtain a pH of 8.3, and the $6.31 \cdot 10^{-5} \text{ mol/L}$ HCl to obtain a pH of 4.2.

In reactor R-2, two reactions take place during acid additions. The acid base reaction between the still present NaOH and HCl, which is converted into NaCl and water, and the precipitation of the proteins after the pH is reduced towards 4.2. In the model, the protein is converted into protein precipitates which differ in M_w and particle size, as depicted in Table 4. The costs analysis for the CISTR reactors R-1 and R-2 have been changed towards the pricing model of Towler et al. [74].

5.3 Centrifugation

To determine the separation percentages during the centrifugation steps, several literature studies will need to be combined. The equipment parameters of the centrifuges are modelled by SuperPro designer according to the Sigma factor of the targeted material, which is affected by the particle size and density [75]. During both the separation step, the density of the targeted component is assumed with a limiting particle diameter equal to half the particle size.

5.3.1 DS-1

The first centrifugation is continuously fed with the basic mixture of R-1, containing the homogenized biomass at elevated pH. The targeted components are the starches, resulting in a limiting particle diameter of 0.65 micron and a density of 1500 kg/m³. The mixture is centrifuged towards a solid concentration of 170 g/L, similar to the retentate concentration of Cavonius et al., where the protein rich fraction from *Nanochloropsis Oculata* was obtained in a similar process [76].

As previously mentioned in section 5.1, the protein solubility after homogenization corrected for elevated pH is equal to 83.916%, resulting in a solid removal percentage of 16.084% [31, 9]. Since chlorophyll is assumed to be bounded to the LHC, the pigment solid removal percentage is set equal to the protein removal percentage [31, 35].

The only study which measured the fatty acid content of each fraction obtained with a similar separation process besides the protein content was based on *Nanochloropsis Oculata* [76]. Despite the significant differences between the lipid content compared to *Chlorella vulgaris*, the behaviour of the lipids during separation are assumed to be comparable [15]. This results in a solid removal percentage of 19% at elevated pH for the PL [76].

Carullo et al. measured the dissolved carbohydrate content of HPH disrupted *Chlorella vulgaris*, which depicted a solubility of 41.9% [77]. Glucose, ash and the salts present in the mixture are assumed to be completely water soluble [44]. Their concentration in the solid stream is dependent on the removed amount of water. With a desired concentration of 170 g/L, this equals 3.18% of the entering amount for each component. Subtracting the glucose from the total solids stream, a separation percentage of 74.92% for starch is required to obtain a total carbohydrate solubility of 41.9% [77]. The solid separation percentages are depicted in Table 11.

Tab. 11: Solid removal percentages for components during DS-1 in mass percentage of the respective component

Components	Solids removed (%)	Ref
PL	19.000%	[76]
Protein	16.084%	[31]
Starch	74.920%	[77]
Glucose	3.180%	
Pigments	16.084%	[35]
Ash	3.180%	
Salts	3.180%	

The separation of the starches into both fractions seems counter-intuitive, since the process is designed to separate solids with a particle diameter above 0.65 micron, half of the starch particle size.

5.3.2 DS-2

After the protein precipitation in R-2, the mixture is loaded into DS-2. Since the precipitated proteins are targeted, the limiting particle diameter is set at 0.5 micron with a density of 1125 kg/m³ [47]. Due to the low density difference between the solid and the fluid combined with the small limited particle, the dewatering of the mixture is being performed in two steps, by centrifugation up until a concentration of 80 g/L, followed by an UF step. The concentration of 80 g/L is used since it equals the maximum input concentration for the VIBRO-filtration units.

The solid removal percentage of the protein precipitate is determined based on the two precipitations

of Ursu et al., which achieved a protein yield of 80% and 78%, and on the work of Cavonius et al., with a yield of 96% of the protein precipitate [35, 76]. The average of these percentages yield protein precipitate removal percentage of 84.6%.

The PL solid removal percentage is based on the second separation step based on *Nanochloropsis Occulta*, which equals 90% [76]. The glucose, ash and salts are assumed to be completely soluble, similar as in DS-1 [44]. For the starches, 77 % of the starches present in the mixture are removed, derived from the normalized figures of Cavonius et al. [76].

5.4 VIBRO-3

To further concentrate the protein fraction, an UF unit with membrane cut-off of 30 kDa is used. This results in the retention of 100% for the remaining starches, the LP present as micelles, and the precipitated proteins and their bounded pigments. Permeation of the glucose, ash and salts is assumed to be possible due to their cut-off sizes and their water solubility.

The filtration unit is modelled in a similar fashion as the other VIBRO UF units. The maximum area equals 27.5 m² per unit with a permeation rate of 14.1 L/hm². Economic modelling of the equipment is based on the VIBRO-I costs model assumptions.

5.5 Spray dryers

During spray drying proteins experience three types of stress, namely heat, mechanical and adsorption to the air-water interface [78, 79]. Since proteins denature with temperature exposures above 30 °C, spray drying of proteins has been approached with caution in the pharmaceutical industry [79]. However, the surface temperature of the droplets after atomisation is kept at wet bulb temperature, significantly lower compared to the drying gas temperature. Since the temperature at the surface of the droplets is limited to the wet bulb temperature, thermal denaturation of the proteins is rarely observed during spray drying [79]. The main source of denaturation in the spray drying of algae is due to the adsorption to the air water interface, which denatures the protein in a similar manner as a water-solvent interface. This can be avoided with the addition of surfactants [80]. During this research, the assumption is made that by keeping the product temperature at a maximum of 30 °C during spray drying no denaturation occurs.

The spray drying conditions of Ruiz et al. are used for the equipment sizing, with an outlet air and product temperature of 100 °C and 30 °C respectively [44]. The specific evaporation rate is set at 100 kg/hm³ with a relative wt water gas/ wt water evap ratio of 20. Inlet air is heated with steam with a temperature of 152 °C. Water is evaporated to a final LOD of 3% in both SDR-1 and SDR-2.

The composition of the dried products CF-1 and PF-1 which are retrieved from SDR-1 and SDR-2 respectively are depicted in Table 12. The protein rich fraction PF-1 of the algae is significantly higher compared to the protein percentages obtained in the onion toppings procedure, indicating a superior product [63]. However, the enriched protein fraction obtained from sugar beet roots is higher compared to the algae, with 74% [8]. Furthermore, the remaining chlorophyll in the algae fraction could limit the usage of the fraction as an ingredient due to its green color [81]. Nonetheless, the nutritional value of the algae fraction is far superior compared to the onion toppings, due to its high protein and lipid content, especially the high PUFA and Omega-3 content of the algae.

Tab. 12: Product composition of algae fractions and onion fractions in wt% of fraction[63]

Component	Algae		Onion toppings	
	PF-1	CF-1	Protein fraction	Fiber fraction
Protein	63.0%	26.0%	24.5%	7.5%
PL	15.5%	7.5%	5.5%	1.0%
Starch	9.5%	59.0%	37.5%	20.0%
Pigments	6.0%	2.5%	n.a.	n.a.
Water	3.0%	3.0%	9.0%	9.0%
Ash	1.5%	1.5%	6.5%	5.5%
Glucose	1.0%	0.5%	n.a.	n.a.
Fibers	n.a.	n.a.	17.5%	57.5%
Salts	0.5%	0.5%	n.a.	n.a.

It must be noted that the carbohydrate fraction is divided differently, with the algae in starches and glucose, whereas the onion toppings divide the carbohydrate fraction into fibers and carbohydrates due to their high cellulose content. Due to the different composition of the CF-1 compared to the fiber rich fraction of the onion toppings, it is difficult to evaluate the product qualities, especially the value. The fiber fraction obtained by Rubisco foods from duckweed and the onion toppings turned out to have beneficial characteristics as a food ingredient. Testing the carbohydrate rich fraction of the algae is required to determine if it has similar properties.

6 Economic evaluation

The economic evaluation of the previously described processes are performed with the SuperPro models, which require several inputs.

The capital investment is divided into the direct, indirect and other costs which are calculated through a distributed set of purchase costs factors. The purchase costs of the spray dryers are based on their SuperPro equipment costs model, whereas the purchase costs of the other equipment used are specified in each section. An additional 20% is added to compensate unlisted equipment purchases.

The direct costs consist of several factors to incorporate piping, instrumentation, insulation, installation building, and auxiliary facilities. Indirect costs consist of engineering and construction costs and are dependent on the direct costs. Finally, the indirect costs, the contractors fee and contingency, are factors of the sum of the direct and indirect costs. The factors are depicted in Table 13. When these factors are combined, the factor between the total capital investments and the purchase costs of the listed equipment is approximately 3.8.

The operational costs consist of the raw materials, labor, facility dependent costs, quality control, waste treatment, consumables, utilities, and rent. The price of the freshwater salts and CO₂ were set at 0.365 and 0.08 €/kg respectively, whereas the water price was set at 0.7 €/m³ STP [82]. The price for HCl and NaOH were set at 0.1 and 0.24 €/kg. Price for operator labor equals 27.6 €/h, derived from figures of Omega Green when assuming a 40 h workweek and a 35 week season. An additional 7.5% of hours are added to incorporate the quality control costs. Water waste treatment was assumed to be performed externally, at a rate of 0.46 €/m³ [44]. Utility costs were unaltered besides the standard power costs, which were set at 0.096 €/kWh [44].

The facility dependent costs consist of the maintenance costs, which are sized on the purchase costs of the equipment, the land lease costs, equaling €80.000/year, and the depreciation of the purchase

Tab. 13: Capital investment costs calculation factors

Direct Costs		Indirect costs	
Piping	0.25	Engineering	0.10
Instrumentation	0.30	Construction	0.20
Insulation	0.01		
Electric facilities	0.05		
Buildings	0.25	Other costs	
Auxiliary facilities	0.35	Contractors fee	0.05
Installation	0.26	Contingency	0.20

costs of the equipment, which are depreciated linearly over a 15 year period. Furthermore, the project lifetime is assumed to be equal to 30 years.

6.1 Economic evaluation of algae production

The maximum production conditions, with 189 kg of biomass per batch with a batch time of 24 h, were used to obtain the equipment sizing. This results in overcapacity during the other production periods, where the additional equipment units are depicted as stand by. The total equipment purchase costs equal €9,212,000, including the unlisted equipment purchases. With the capital investment factors depicted in Table 13, this results in a total investment of €34,952,000.

Material consumption and operating conditions are modelled with the average production of the 35 week season, at 125 kg/batch with a batch time of 29.5 h. This resulted in salt consumption of 102 kg/batch, a water consumption of 51.83 m³/batch including the cooling water of the spray cooler, and a CO₂ consumption of 69.59 kg/batch. During the simulation, the bioreactor initialises with its content of the previous simulation since only 30% of the volume is removed. The remaining 70% is seen as a new raw material by SuperPro, resulting in hugely inflated consumption. This is prevented by changing the input water into stock mixture H₂O which solely consists of water. During the simulation of the algae production, the stock mixture H₂O has a price of 0.70 €/m³, whereas the price for water is set at 0 such that the economic evaluation of SuperPro remains valid and water consumption can be evaluated by the stock mixture H₂O consumption. In Appendix A, the stock mixture H₂O is depicted as water which has been altered afterwards.

The summary of the costs are depicted in Table 14, whereas the details are depicted in Appendix A.

Tab. 14: Summary of Economic evaluation of algae production

Total investment		€ 34,952,000
Operating costs		€ 7,154,000
Biomass production	(MT)	904
	€/kg	€ 7.92
PROD-1 production	(MT)	37517
	€/kg	€ 0.19

The main contributors of the operating costs are the facility dependent costs, the consumables, and the labor costs, with 36%, 25%, and 21% respectively. Both the facility dependent costs and the consumables are related to the equipment selection, their consumables, and their respective costs. The bioreactor and the LDPE bags have been developed to be as cost effective as possible by

Omega Green. Furthermore, with an assumed cost reduction of 20% concerning the LDPE bags due to upscaling leaves little promise for further reduction of the equipment and consumables costs for the bioreactor. The majority of the equipment costs are attributed to the VIBRO filtration units. The novel technology shows promise in its energy usage, but is accompanied by high purchase costs. Switching to other dewatering techniques might reduce the facility dependent and consumables costs, but is likely to increase the consumption of utilities.

It is necessary to keep in mind the degree of dewatering with the production costs per kg of biomass. The expected price of 7.92 €/kg of biomass is relatively low compared to other studies [44, 83]. However, at 24 g/L the algae are far from being completely dried. The price of 7.92 €/kg of biomass translates to production costs of the PROD-1 stream of 0.19€/kg.

6.2 Economic evaluation of the downstream processing

During the economic evaluation of the downstream processing, two scenario's will be evaluated. During the first scenario, the equipment is sized according to the maximum production of the algae. The operating time is equal to the production time of 5880 h, all algae produced is immediately refined into the two fractions. In the second scenario, the possibility for drying and storage of whole algae is investigated to prolong the refinement campaign towards 7920 h, reducing the average throughput.

6.2.1 Scenario 1

With a campaign time of 5880 h, the input of the refinement process PROD-1 equals 6.272 MT/h and 11.613 MT/h during average and maximal production respectively. At maximum throughput, the purchase costs of the equipment equal €1,873,000, translating to a total investment of €7,306,000.

In contrast to the algae production, the raw materials consumption is insignificant during the refinery steps. Due to the mild conditions of the process, only a small annual amount of NaOH and HCl is used, resulting in material a consumption cost of €1,000. 94% of the operating costs can be attributed towards labor, utilities and facility dependent costs. The high utility costs are caused by the homogenization method, which consumes 80 m³ of chilled water and 550 kW. Combined with the other equipment, the annual demand for power, chilled water and steam equals 4769007 kWh, 559826 MT, and 6239 MT respectively, resulting in utility costs of €757,000, 33% of the operating costs. Switching towards another homogenization method might reduce costs related to the utilities, but is likely to increase other costs as can be seen with bead milling in section 5.1. The total annual operating costs for the S1 section equals €2,306,000.

To calculate the revenue, a price for the protein rich fraction (PF-1) and the carbohydrate rich fraction (CF-1) needs to be determined. Expected prices for PF-1 and CF-1 range from 10-25 €/kg and 5-10 €/kg respectively. The optimistic expected price is set at 85 % of the maximum price, 21.25 €/kg and 8.50 €/kg for PF-1 and CF-1 respectively.

The summary of the costs and revenues are depicted in Table 15, whereas the details are depicted in Appendix B.

With the optimistic pricing used for both the products, a ROI of 36% is achieved after 30 years. A positive return of investment is obtained at prices above 20.83 €/kg and 8.12 €/kg for PF-1 and CF-1 respectively, equalling to 81.23% of the expected maximum price. The majority of the costs are related to the algae production, with 83% of the total investment and 76% of the operating costs.

Tab. 15: Economic evaluation of algae production and refinery S1 with ROI over complete project lifetime

	Algae production	S1	Total
Total investment	€ 34,952,000	€ 7,306,000	€ 42,258,000
Operating Costs	€ 7,154,000	€ 2,287,000	€ 9,441,000
Revenues			
PF-1		€ 9,304,000.00	
CF-1		€ 2,067,000.00	
Total revenues			€ 11,371,000
Gross margin			17%
Payback time (yr)			22.00
ROI			37%

6.2.2 Scenario 2

By prolonging the campaign period of the refinery process by incorporating a drying and storage process to spread the overproduction during the summer, the investment costs are expected to decrease. This reduction will be profitable when both the investment costs and operating costs of the additional drying section are lower.

To figure out the costs of drying and storage, four initial parameters are needed to model the drying procedure. The duration at which drying is required, the required capacity, the average drying rate, and the average retention period of the stored algae. Furthermore, the type of drying process needs to be determined. The yearly production, consumption and the storage of the algae is visualized in Figure 4.

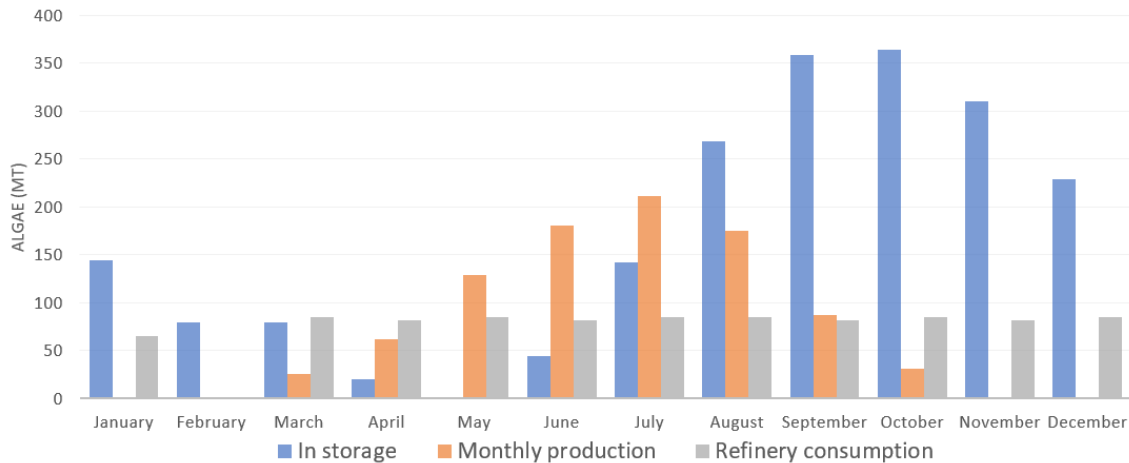


Fig. 4: Visualization of yearly production of algae, refinery consumption during during a 7920 h season, and the algae in storage

The process time for the drying procedure can be derived from Figure 4. The monthly production exceeds the refinery consumption in the months May up until September, equalling a campaign of 3672 h. The average algae consumption in the refinery equals 2.7 MT/day when a 7920 h season is assumed. The difference between the monthly production and the refinery consumption is at its maximum in July, at 169 kg/h, whereas the average of the overproduction equals 99.2 kg/h. The storage capacity must be equal to 364 MT which is required at the start of October. The average

retention time was estimated at 173 days (first in first out).

In order to store the algae to prolong the refinery season, the product needs to be dried. Several drying methods are available. Freeze-drying is the most suitable drying method to maintain the nutrient and bioactive components present in *Chlorella vulgaris*. Experiments concerning freeze drying did not result in any significant degradation of the protein [84]. However, due to the low capacity and high labor intensity, freeze drying will result in high investment and operational costs. Spray drying of *Spirulina* resulted in a 10% protein loss, which would result in reduced production of the desired end product [85]. Furthermore, spray drying will require significant amounts of heat. Other industrial drying techniques such as convective drying or thin layer drying have shown to result into higher degradation compared to spray drying [85]. Solar drying techniques, which could be an interesting drying technique due to its energy neutral nature, have been shown to be ineffective in central Europe due to environmental temperatures and the required labor, which is elaborated on in Appendix D. The choice was made to model the drying procedure with spray drying.

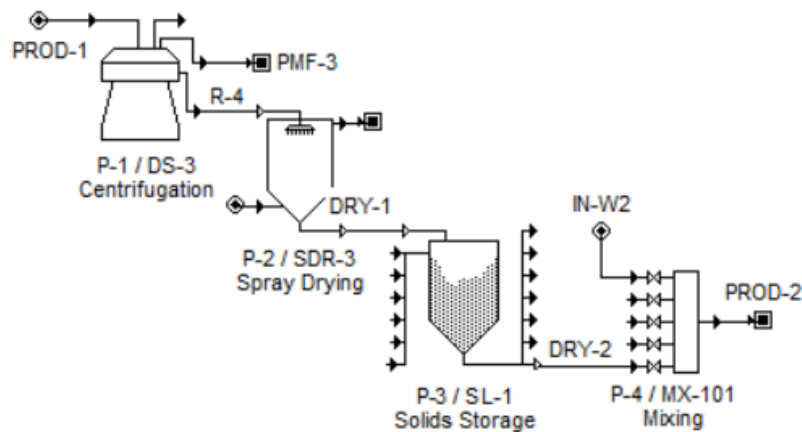


Fig. 5: Algae drying procedure of overproduction through spray drying

The drying procedure of the process is depicted in Figure 5. The disk-stack centrifuge is used for dewatering the algae towards 180 g/L before it is dried with the spray dryer SDR-3. The spray dryer uses similar assumptions as previously modelled spray dryers, whereas the centrifuge assumes a biomass particle diameter of 5 micron. After drying, the solids are stored in a silo which keeps the temperature of the material below 20 °C. After the average residence time of 173 days, the product is removed from storage and mixed with water at a biomass concentration of 24 g/L which is transported to the refinery.

The overall effect on the water consumption of the drying procedure is minimal. PMF-3 is recycled into the algae production storage, lowering water and salt consumption which can be used in IN-W2 for water addition. The only additional water required is the water leaving SDR-3, at a rate of 480 kg/h equalling to 1768 m³ annually.

Tab. 16: Economic evaluation of algae production, drying procedure and refinery S2 with ROI over complete project lifetime

	Algae production	Drying	S2	Total
Total investment	€ 34,952,000	€ 2,536,000	€ 4,805,000	€ 42,293,000
Operating Costs	€ 7,154,000	€ 545,000	€ 2,403,000	€ 10,102,000
Revenues				
PF-1			€ 9,303,000	
CF-1			€ 2,067,000	
Total revenues				€ 11,370,000
Gross margin				11%
Payback time (yr)				33.00
ROI				-10%

When looking at the results depicted in Table 16, it is noticeable that the second scenario is inferior compared to the first scenario. With the same pricing, the gross margin reduces by 5%, resulting in a negative ROI with the same optimistic pricing. Prolonging the campaign period of the refinery process by the introduction of a drying procedure has reduced the investment costs of the refinery S2 by €2,500,000. However, this is compensated by the required investment costs of the drying procedure. The operational costs of S2 have increased compared to S1. Where the reduction of the equipment price of S2 resulted in a significant decrease in facility dependent and consumable costs as depicted in Appendix D, the extended campaign resulted in increased labor dependent costs. Furthermore, the operating costs of the drying procedure further reduce the gross margin.

It must be noted that the possible degradation of the algae during drying and storage is ignored [85]. Incorporating the degradation would further reduce the profitability of the scenario, meaning the results in Table 16 can be considered as an upper limit. Overall, it can be concluded that the addition of a drying procedure does not result in increased performance of the process.

7 Discussion

The algae production combined with the refinery of scenario 1 has the potential to result in a profitable process. With a relatively simple refinery process, requiring a limited investment compared to the required production investment, the process is able to produce a protein rich fraction suitable for formulated foods. This will result in an increased market size for the product compared to the whole algae market. However, quite some uncertainties are still present.

The pricing indications of the products were retrieved from conversations of Omega Green with Rubisco Foods. The assumed optimistic pricing is likely to be overestimated. Due to the quality of the protein fraction in terms of nutritional value and protein content compared to the onion fraction of Rubisco Foods, the optimistic pricing of this fraction might be valid. With a similar protein content as the product of Cosun, the fraction is likely to have excellent functional properties, such as good solubility, emulsifying capabilities, and gelling behavior, making it a high value product. This makes the optimistic pricing of the fraction justifiable. However, for the carbohydrate fraction, it is nearly impossible to determine the quality of the product. The fiber fractions derived from the onion toppings and duckweed differ significantly in their constituents compared to the carbohydrate rich fraction of the algae [63, 56]. Due to the low cellulose content of the algae, which is only present in the cell wall [51], it might lack the properties of the fiber fraction. This uncertainty makes the optimistic pricing at 85% of the maximum price unlikely.

A reduction of the price for carbohydrate fraction will have an profound effect on the profitability of the project, where a price below 6.4 €/kg will result in a negative ROI when the pricing of the protein fraction is left unaltered at 21.25 €/kg. This shows the uncertainty in this research regarding the economic evaluation of this process.

Improvements concerning the algae production process can mainly be found in the dewatering technologies. The VIBRO-I technology, although being energy efficient, is accompanied by high investment and consumable costs. If the decision is made to purchase the pilot unit of SANI-membranes, test concerning the durability of the membranes might reduce the assumed consumable costs, whereas accurate energy consumption measurements could possibly further reduce the utility consumption.

The choices concerning the homogenization method were based on the accompanied costs and the high effectiveness of the methods. Due to the high utility consumption of the HPH process, other homogenization methods could be deemed more suitable through other selection criteria. Each homogenization method is accompanied by its own disadvantages and is likely to remain a significant portion of the refinery costs.

Furthermore, to increase the validity of the model, detailed information on energy consumption of the current process needs to be incorporated. The power consumption in the model is based on overall consumption figures of the production processes. Detailed information on the power consumption could increase the accuracy during upscaling, which might reduce the required energy.

8 Conclusion

A 40 hectare algae production plant which utilizes the Omega Green algae production system was able to produce and dewater *Chlorella vulgaris* towards 24 g/L at 7.92 €/kgDW. The introduction of a mild refinery process resulted into a dried functional protein rich fraction and a dried carbohydrate rich fraction. Feasibility studies were performed according to two scenarios, in which the introduction of a drying step to prolong the refinery season was deemed unprofitable. A positive ROI is achieved with prices above 20.83 €/kg and 8.12 €/kg for the protein rich and carbohydrate rich fraction respectively. At the optimistic pricing of 21.25 €/kg and 8.50 €/kg for the protein and carbohydrate fraction, a gross margin of 17% results into a ROI of 37% with a payback time of 22 years. This results in weak business case which is unlikely to attract investors. Overall, the introduction of a mild refinery process can be achieved with relatively limited investment costs compared to the investment needed for the algae production. This process is able to convert the whole algae into fractions suitable to be used in formulated foods for human consumption, creating new markets which can be targeted. Nonetheless, the process will not be economically feasible.

References

- [1] Groningen Seaports. Port handbook, accessed 31 August 2020. <https://www.groningen-seaports.com/wp-content/uploads/GSP-PortHandbook-VII.pdf>.
- [2] Jiri Hartog. Voorbereidingen grootschalig algenkweekcentrum delfzijl. 2017.
- [3] Miguel Olaizola and Claudia Grewe. Commercial microalgal cultivation systems. In *Grand Challenges in Algae Biotechnology*, pages 3–34. Springer, 2019.
- [4] Rene B Draaisma, Rene H Wijffels, PM Ellen Slegers, Laura B Brentner, Adip Roy, and Maria J Barbosa. Food commodities from microalgae. *Current opinion in biotechnology*, 24(2):169–177, 2013.
- [5] Edgar Suarez Garcia, Giuseppe Olivieri, Lolke Sijtsma, Marian H Vermuë, Maria Barbosa, J Hans Reith, Corjan van den Berg, Michel HM Eppink, and René H Wijffels. Integrated biorefineries for algal biomolecules. In *Grand Challenges in Algae Biotechnology*, pages 293–317. Springer, 2019.
- [6] Groningen Seaports. Wat doen we om de havenvisie te realiseren en waar staan we in 2018, accessed 31 August 2020. <https://strategie.groningen-seaports.com/havenvisie-2030/voortgang-havenvisie/>.
- [7] José L García, Marta de Vicente, and Beatriz Galán. Microalgae, old sustainable food and fashion nutraceuticals. *Microbial Biotechnology*, 10(5):1017–1024, 2017.
- [8] Mathijs Grootsholten, Micheal Litjens, Andre de Haan, Harmen de Jong, Maria van Gorp, and Wilco Duvivier. Beet protein compositions, production thereof and use thereof in formulated food systems, 2019.
- [9] Emma Teuling, Peter A Wierenga, Johan W Schrama, and Harry Gruppen. Comparison of protein extracts from various unicellular green sources. *Journal of agricultural and food chemistry*, 65(36):7989–8002, 2017.
- [10] Jafar Seyfabadi, Zohreh Ramezanzpour, and Zahra Amini Khoeyi. Protein, fatty acid, and pigment content of chlorella vulgaris under different light regimes. *Journal of Applied Phycology*, 23(4):721–726, 2011.
- [11] Amos Richmond and Qiang Hu. *Handbook of microalgal culture: applied phycology and biotechnology*. John Wiley & Sons, 2013.
- [12] Kun Zhang, Bingjie Sun, Xingxing She, Fengmin Zhao, Youfu Cao, Difeng Ren, and Jun Lu. Lipid production and composition of fatty acids in chlorella vulgaris cultured using different methods: photoautotrophic, heterotrophic, and pure and mixed conditions. *Annals of microbiology*, 64(3):1239–1246, 2014.
- [13] R Sindhu, RO Rajesh, TK Godan, P Binod, and A Pandey. Bioengineering advancements, innovations and challenges on green synthesis of 2, 5-furan dicarboxylic acid. *Bioengineered*, 2019.
- [14] Seyedeh Fatemeh Sajadian, Mohammad Hossein Morowvat, and Younes Ghasemi. Investigation of autotrophic, heterotrophic, and mixotrophic modes of cultivation on lipid and biomass production in chlorella vulgaris. *National Journal of Physiology, Pharmacy and Pharmacology*, 8(4):594–599, 2018.

- [15] Ö Tokuşoglu and MK Ünal. Biomass nutrient profiles of three microalgae: *Spirulina platensis*, *Chlorella vulgaris*, and *Isochrysis galbana*. *Journal of food science*, 68(4):1144–1148, 2003.
- [16] Yasmin Anum Mohd Yusof, Junaida Maimunah Hassan Basari, Nor Ashikeen Mukti, Razali Sabuddin, A Razak Muda, Suhaina Sulaiman, Suzana Makpol, and Wan Zurinah Wan Ngah. Fatty acids composition of microalgae *Chlorella vulgaris* can be modulated by varying carbon dioxide concentration in outdoor culture. *African Journal of Biotechnology*, 10(62):13536–13542, 2011.
- [17] Yanna Liang, Nicolas Sarkany, and Yi Cui. Biomass and lipid productivities of *Chlorella vulgaris* under autotrophic, heterotrophic and mixotrophic growth conditions. *Biotechnology letters*, 31(7):1043–1049, 2009.
- [18] İlknur Ak, Semra Cirik, and Tolga Goksan. Effects of light intensity, salinity and temperature on growth in camalti strain of *Dunaliella viridis* teodoresco from turkey. *J Biol Sci*, 8(8):1356–1359, 2008.
- [19] Hendrik Poorter, Ülo Niinemets, Nikolaos Ntagkas, Alrun Siebenkäs, Maarit Mäenpää, Shizue Matsubara, and ThijsL Pons. A meta-analysis of plant responses to light intensity for 70 traits ranging from molecules to whole plant performance. *New Phytologist*, 223(3):1073–1105, 2019.
- [20] Melinda J Griffiths, Robert P van Hille, and Susan TL Harrison. The effect of nitrogen limitation on lipid productivity and cell composition in *Chlorella vulgaris*. *Applied microbiology and biotechnology*, 98(5):2345–2356, 2014.
- [21] Jian-Ming Lv, Li-Hua Cheng, Xin-Hua Xu, Lin Zhang, and Huan-Lin Chen. Enhanced lipid production of *Chlorella vulgaris* by adjustment of cultivation conditions. *Bioresource technology*, 101(17):6797–6804, 2010.
- [22] Mathias Ahii Chia, Ana Teresa Lombardi, Maria Da Graça Gama Melão, and Christopher C Parrish. Effects of cadmium and nitrogen on lipid composition of *Chlorella vulgaris* (trebouxiophyceae, chlorophyta). *European Journal of Phycology*, 48(1):1–11, 2013.
- [23] Mathias Ahii Chia, Ana Teresa Lombardi, G Melão Maria da Graça, and Christopher C Parrish. Lipid composition of *Chlorella vulgaris* (trebouxiophyceae) as a function of different cadmium and phosphate concentrations. *Aquatic Toxicology*, 128:171–182, 2013.
- [24] Kwang Hyun Cha, Hee Ju Lee, Song Yi Koo, Dae-Geun Song, Dong-Un Lee, and Cheol-Ho Pan. Optimization of pressurized liquid extraction of carotenoids and chlorophylls from *Chlorella vulgaris*. *Journal of agricultural and food chemistry*, 58(2):793–797, 2010.
- [25] Kiwa Kitada, Siti Machmudah, Mitsuru Sasaki, Motonobu Goto, Yuya Nakashima, Shoichiro Kumamoto, and Takashi Hasegawa. Supercritical CO₂ extraction of pigment components with pharmaceutical importance from *Chlorella vulgaris*. *Journal of Chemical Technology & Biotechnology: International Research in Process, Environmental & Clean Technology*, 84(5):657–661, 2009.
- [26] Luz E De-Bashan, Yoav Bashan, Manuel Moreno, Vladimir K Lebsky, and Jose J Bustillos. Increased pigment and lipid content, lipid variety, and cell and population size of the microalgae *Chlorella* spp. when co-immobilized in alginate beads with the microalgae-growth-promoting bacterium *Azospirillum brasilense*. *Canadian journal of microbiology*, 48(6):514–521, 2002.
- [27] Dale D McClure, Jonathan K Nightingale, Audrey Luiz, Sachin Black, Jingyuan Zhu, and

- John M Kavanagh. Pilot-scale production of lutein using *chlorella vulgaris*. *Algal Research*, 44:101707, 2019.
- [28] Weibao Kong, Shuling Yang, Hui Wang, Huanran Huo, Baomin Guo, Na Liu, Aimei Zhang, and Shiquan Niu. Regulation of biomass, pigments, and lipid production by *chlorella vulgaris* 31 through controlling trophic modes and carbon sources. *Journal of Applied Phycology*, pages 1–11, 2020.
- [29] Blanca Araya, Luísa Gouveia, Beatriz Nobre, Alberto Reis, Rolando Chamy, and Paola Poirrier. Evaluation of the simultaneous production of lutein and lipids using a vertical alveolar panel bioreactor for three *chlorella* species. *Algal Research*, 6:218–222, 2014.
- [30] Mengyue Gong and Amarjeet Bassi. Investigation of *chlorella vulgaris* utex 265 cultivation under light and low temperature stressed conditions for lutein production in flasks and the coiled tree photo-bioreactor (ctpbr). *Applied biochemistry and biotechnology*, 183(2):652–671, 2017.
- [31] Sayali Kulkarni and Zivko Nikolov. Process for selective extraction of pigments and functional proteins from *chlorella vulgaris*. *Algal research*, 35:185–193, 2018.
- [32] microganic. *FitFeed Chlorella Powder*, 2020.
- [33] Andreia S Ferreira, Sónia S Ferreira, Alexandra Correia, Manuel Vilanova, Tiago H Silva, Manuel A Coimbra, and Cláudia Nunes. Reserve, structural and extracellular polysaccharides of *chlorella vulgaris*: A holistic approach. *Algal Research*, 45:101757, 2020.
- [34] JM Bailey and AC Neish. Starch synthesis in *chlorella vulgaris*. *Canadian Journal of Biochemistry and Physiology*, 32(4):452–464, 1954.
- [35] Alina-Violeta Ursu, Alain Marcati, Thierry Sayd, Véronique Sante-Lhoutellier, Gholamreza Djelveh, and Philippe Michaud. Extraction, fractionation and functional properties of proteins from the microalgae *chlorella vulgaris*. *Bioresource technology*, 157:134–139, 2014.
- [36] Xin Wang, Zhouyuan Shen, and Xiaoling Miao. Nitrogen and hydrophosphate affects glycolipids composition in microalgae. *Scientific reports*, 6:30145, 2016.
- [37] Daniel A White, Paul A Rooks, Susan Kimmance, Karen Tait, Mark Jones, Glen A Tarran, Charlotte Cook, and Carole A Llewellyn. Modulation of polar lipid profiles in *chlorella* sp. in response to nutrient limitation. *Metabolites*, 9(3):39, 2019.
- [38] Dirk Willem Van Krevelen and Klaas Te Nijenhuis. *Properties of polymers: their correlation with chemical structure; their numerical estimation and prediction from additive group contributions*. Elsevier, 2009.
- [39] Patrizio Raffa. *Interfacial Engineering A multidisciplinary approach*. Unpublished, 2019.
- [40] Edwin N Frankel, Teresa Satué-Gracia, Anne S Meyer, and J Bruce German. Oxidative stability of fish and algae oils containing long-chain polyunsaturated fatty acids in bulk and in oil-in-water emulsions. *Journal of Agricultural and Food Chemistry*, 50(7):2094–2099, 2002.
- [41] Fereidoon Shahidi and Ying Zhong. Lipid oxidation and improving the oxidative stability. *Chemical society reviews*, 39(11):4067–4079, 2010.
- [42] Yan Shen, Ting Lu, Xiao-Yang Liu, Man-Tong Zhao, Fa-Wen Yin, Kanyasiri Rakariyatham,

- and Da-Yong Zhou. Improving the oxidative stability and lengthening the shelf life of dha algae oil with composite antioxidants. *Food Chemistry*, 313:126139, 2020.
- [43] Simon M Loveday. Food proteins: technological, nutritional, and sustainability attributes of traditional and emerging proteins. *Annual review of food science and technology*, 10:311–339, 2019.
- [44] Jesús Ruiz, Giuseppe Olivieri, Jeroen de Vree, Rouke Bosma, Philippe Willems, J Hans Reith, Michel HM Eppink, Dorinde MM Kleinegris, René H Wijffels, and Maria J Barbosa. Towards industrial products from microalgae. *Energy & Environmental Science*, 9(10):3036–3043, 2016.
- [45] Harold P Erickson. Size and shape of protein molecules at the nanometer level determined by sedimentation, gel filtration, and electron microscopy. *Biological procedures online*, 11(1):32, 2009.
- [46] DJ Bell, D Heywood-Waddington, M Hoare, and P Dunnill. The density of protein precipitates and its effect on centrifugal sedimentation. *Biotechnology and bioengineering*, 24(1):127–141, 1982.
- [47] DYM Lui, JD Litster, and ET White. Precipitation of soy proteins: particle formation and protein separation. *AIChE journal*, 53(2):514–522, 2007.
- [48] M Martínez-Aragón, S Burghoff, ELV Goetheer, and AB de Haan. Guidelines for solvent selection for carrier mediated extraction of proteins. *Separation and purification technology*, 65(1):65–72, 2009.
- [49] Theodore T Herskovits, Barbara Gadegbeku, and Helen Jaillet. On the structural stability and solvent denaturation of proteins i. denaturation by the alcohols and glycols. *Journal of Biological Chemistry*, 245(10):2588–2598, 1970.
- [50] Ciarán Ó Fágáin. Understanding and increasing protein stability. *Biochimica et Biophysica Acta (BBA)-Protein Structure and Molecular Enzymology*, 1252(1):1–14, 1995.
- [51] Mina Makooi, John T Reynolds, and HW Johansen. Effects of glucose and light on cellulose content of chlorella pyrenoidosa. *Phytochemistry*, 15(3):367–369, 1976.
- [52] I Gifuni, Giuseppe Olivieri, I Russo Krauss, G D’Errico, A Pollio, and A Marzocchella. Microalgae as new sources of starch: isolation and characterization of microalgal starch granules. *Chemical Engineering Transactions*, 57:1423–1428, 2017.
- [53] Rupendra Mukerjea, Giles Slocum, and John F Robyt. Determination of the maximum water solubility of eight native starches and the solubility of their acidic-methanol and-ethanol modified analogues. *Carbohydrate research*, 342(1):103–110, 2007.
- [54] Keshun Liu. Characterization of ash in algae and other materials by determination of wet acid indigestible ash and microscopic examination. *Algal research*, 25:307–321, 2017.
- [55] Lutz Grossmann, Jörg Hinrichs, and Jochen Weiss. Cultivation and downstream processing of microalgae and cyanobacteria to generate protein-based technofunctional food ingredients. *Critical reviews in food science and nutrition*, pages 1–29, 2019.
- [56] Laurent Olivier, Paul Antalik, and Brandi Alderson. Method and system for processing of aquatic species, 2012.

- [57] Roelof Schipperus, J Spruijt-Verkerke, and RY van der Weide. Energierijk: Deelproject algenteelt. Technical report, PPO AGV, 2013.
- [58] Joanneke Spruijt, Roelof Schipperus, AMJ Kootstra, and CLM de Visser. Algaeconomics: bio-economic production models of micro-algae and downstream processing to produce bio energy carriers. Technical report, EnAlgae Swansea University, 2015.
- [59] Jiří Doucha, František Straka, and Karel Lívanský. Utilization of flue gas for cultivation of microalgae (*Chlorella* sp.) in an outdoor open thin-layer photobioreactor. *Journal of Applied Phycology*, 17(5):403–412, 2005.
- [60] John Sheehan, Terri Dunahay, John Benemann, and Paul Roessler. A look back at the us department of energy’s aquatic species program: biodiesel from algae. *National Renewable Energy Laboratory*, 328:1–294, 1998.
- [61] SANI Membranes. Vibro-i specification sheet, accessed 14 september 2020. <https://sanimembranes.com/onewebmedia/Vibro-I%20Product%20Sheet.pdf>.
- [62] SANI Membranes. Disruptive filtration solutions, accessed 14 september 2020. https://mejeritekniskselskab.dk/sites/default/files/dms/Seminarprogrammer/henrik_hjelmsmark_sani_membranes_dairy_04062018.pdf.
- [63] Johannes Derksen and Laurent Zwart. Protein composition obtained from allium, 2017.
- [64] AM Abo-Shady, YA Mohamed, and T Lasheen. Chemical composition of the cell wall in some green algae species. *Biologia plantarum*, 35(4):629–632, 1993.
- [65] Hongli Zheng, Jilong Yin, Zhen Gao, He Huang, Xiaojun Ji, and Chang Dou. Disruption of *Chlorella vulgaris* cells for the release of biodiesel-producing lipids: a comparison of grinding, ultrasonication, bead milling, enzymatic lysis, and microwaves. *Applied biochemistry and biotechnology*, 164(7):1215–1224, 2011.
- [66] Mohammed Shehadul Islam, Aditya Aryasomayajula, and Ponnambalam Ravi Selvaganapathy. A review on macroscale and microscale cell lysis methods. *Micromachines*, 8(3):83, 2017.
- [67] Kuan-Yeow Show, Duu-Jong Lee, Joo-Hwa Tay, Tse-Min Lee, and Jo-Shu Chang. Microalgal drying and cell disruption—recent advances. *Bioresource technology*, 184:258–266, 2015.
- [68] Sergio I Martínez-Monteagudo, Bing Yan, and VM Balasubramaniam. Engineering process characterization of high-pressure homogenization—from laboratory to industrial scale. *Food Engineering Reviews*, 9(3):143–169, 2017.
- [69] L Grossmann, S Ebert, J Hinrichs, and J Weiss. Effect of precipitation, lyophilization, and organic solvent extraction on preparation of protein-rich powders from the microalgae *Chlorella protothecoides*. *Algal research*, 29:266–276, 2018.
- [70] Carl Safi, Christine Frances, Alina Violeta Ursu, Céline Laroche, Cécile Pouzet, Carlos Vaca-Garcia, and Pierre-Yves Pontalier. Understanding the effect of cell disruption methods on the diffusion of *Chlorella vulgaris* proteins and pigments in the aqueous phase. *Algal research*, 8:61–68, 2015.
- [71] PR Postma, E Suarez-Garcia, Carl Safi, K Yonathan, G Olivieri, MJ Barbosa, Rene Hubertus Wijffels, and MHM Eppink. Energy efficient bead milling of microalgae: Effect of bead size on disintegration and release of proteins and carbohydrates. *Bioresource technology*, 224:670–679, 2017.

- [72] Qi Luo, Wenting Zhan, Remko M Boom, and Anja EM Janssen. Interactions between acid and proteins under in vitro gastric condition—a theoretical and experimental quantification. *Food & function*, 9(10):5283–5289, 2018.
- [73] Yamile A Mennah-Govela, R Paul Singh, and Gail M Bornhorst. Buffering capacity of protein-based model food systems in the context of gastric digestion. *Food & function*, 10(9):6074–6087, 2019.
- [74] Gavin Towler and Ray Sinnott. *Chemical engineering design: principles, practice and economics of plant and process design*. Elsevier, 2012.
- [75] Charles M Ambler. The fundamentals of separation, including sharples “sigma value” for predicting equipment performance. *Ind. Eng. Chem*, 53(6):430–433, 1961.
- [76] Lillie R Cavonius, Eva Albers, and Ingrid Undeland. ph-shift processing of nannochloropsis oculata microalgal biomass to obtain a protein-enriched food or feed ingredient. *Algal research*, 11:95–102, 2015.
- [77] Daniele Carullo, Biresaw Demelash Abera, Alessandro Alberto Casazza, Francesco Donsi, Patrizia Perego, Giovanna Ferrari, and Gianpiero Pataro. Effect of pulsed electric fields and high pressure homogenization on the aqueous extraction of intracellular compounds from the microalgae chlorella vulgaris. *Algal research*, 31:60–69, 2018.
- [78] Yuh-Fun Maa and Steven J Prestrelski. Biopharmaceutical powders particle formation and formulation considerations. *Current pharmaceutical biotechnology*, 1(3):283–302, 2000.
- [79] Morten Jonas Maltesen and Marco Van De Weert. Drying methods for protein pharmaceuticals. *Drug Discovery Today: Technologies*, 5(2-3):e81–e88, 2008.
- [80] Serena D Webb, Stephen L Golledge, Jeffrey L Cleland, John F Carpenter, and Theodore W Randolph. Surface adsorption of recombinant human interferon- γ in lyophilized and spray-lyophilized formulations. *Journal of pharmaceutical sciences*, 91(6):1474–1487, 2002.
- [81] B Klamczynska and WD Mooney. Heterotrophic microalgae: a scalable and sustainable protein source. In *Sustainable protein sources*, pages 327–339. Elsevier, 2017.
- [82] Waterbedrijf Groningen. Tarieven grootverbruk 2020, 2020.
- [83] Jeroen H de Vree. *Outdoor production of microalgae*. PhD thesis, Wageningen University, 2016.
- [84] Marina Stramarkou, Sofia Papadaki, Konstantina Kyriakopoulou, and Magdalini Krokida. Effect of drying and extraction conditions on the recovery of bioactive compounds from chlorella vulgaris. *Journal of Applied Phycology*, 29(6):2947–2960, 2017.
- [85] Fábio de Farias Neves, Mariana Demarco, and Giustino Tribuzi. Drying and quality of microalgal powders for human alimentation. In *Microalgae-From Physiology to Application*. IntechOpen, 2019.
- [86] Abhay Bhanudas Lingayat, VP Chandramohan, VRK Raju, and Venkatesh Meda. A review on indirect type solar dryers for agricultural crops—dryer setup, its performance, energy storage and important highlights. *Applied Energy*, 258:114005, 2020.
- [87] A Esper and W Mühlbauer. Solar drying—an effective means of food preservation. *Renewable energy*, 15(1-4):95–100, 1998.

- [88] Darshit Parikh and GD Agrawal. Solar drying in hot and dry climate of jaipur. *International Journal of Renewable Energy Research (IJRER)*, 1(4):224–231, 2012.
- [89] Ahmad Fudholi, Kamaruzzaman Sopian, B Bakhtyar, Mohamed Gabbasa, Mohd Yusof Othman, and Mohd Hafidz Ruslan. Review of solar drying systems with air based solar collectors in malaysia. *Renewable and Sustainable Energy Reviews*, 51:1191–1204, 2015.
- [90] David B Ampratwum and Atsu SS Dorvlo. Evaluation of a solar cabinet dryer as an air-heating system. *Applied Energy*, 59(1):63–71, 1998.
- [91] Ahmad Fudholi, Kamaruzzaman Sopian, Mohd Yusof Othman, and Mohd Hafidz Ruslan. Energy and exergy analyses of solar drying system of red seaweed. *Energy and Buildings*, 68:121–129, 2014.
- [92] J Banout, P Ehl, J Havlik, B Lojka, Z Polesny, and V Verner. Design and performance evaluation of a double-pass solar drier for drying of red chilli (*capsicum annum l.*). *Solar energy*, 85(3):506–515, 2011.
- [93] PN Sarsavadia. Development of a solar-assisted dryer and evaluation of energy requirement for the drying of onion. *Renewable energy*, 32(15):2529–2547, 2007.
- [94] MW Kareem, Khairul Habib, MH Ruslan, and Bidyut Baran Saha. Thermal performance study of a multi-pass solar air heating collector system for drying of roselle (*hibiscus sabdariffa*). *Renewable Energy*, 113:281–292, 2017.
- [95] Erick Cesar López-Vidaña, Lilia L Méndez-Lagunas, and Juan Rodríguez-Ramírez. Efficiency of a hybrid solar–gas dryer. *Solar energy*, 93:23–31, 2013.
- [96] BMA Amer, MA Hossain, and K Gottschalk. Design and performance evaluation of a new hybrid solar dryer for banana. *Energy conversion and management*, 51(4):813–820, 2010.
- [97] MA Hossain, BMA Amer, and K Gottschalk. Hybrid solar dryer for quality dried tomato. *Drying Technology*, 26(12):1591–1601, 2008.
- [98] S Boughali, H Benmoussa, B Bouchekima, D Mennouche, H Bouguettaia, and D Bechki. Crop drying by indirect active hybrid solar–electrical dryer in the eastern algerian septentrional sahara. *Solar energy*, 83(12):2223–2232, 2009.
- [99] Franz Emminger. Belt dryer and method for dewatering microalgae, November 26 2019. US Patent 10,488,110.

A Appendix A: Algae Production economic evaluation

Annual Operating Costs Algae Production

Operating Costs	Annual Cost (€)	%
Raw Materials	€ 775,000	11%
Labor-Dependent	€ 1,500,000	21%
Facility-Dependent	€ 2,582,000	36%
Laboratory/QC/QA	€ 113,000	2%
Consumables	€ 1,755,000	25%
Waste	€ 40,000	1%
Utilities	€ 279,000	4%
Miscellaneous	€ 80,000	1%
TOTAL	€ 7,154,000	

Material Cost

Bulk Material	Unit Cost (€)	Annual Amount	Annual Cost (€)	%
Alga sweetwater salts	0.36	814088 kg	€ 293,072	38%
Carb. Dioxide	0.08	2405021 kg	€ 192,402	25%
Water	0.70	413383 m3(STP)	€ 289,368	37%
TOTAL			€ 774,841	100.00

Labor Cost

Labor Type	Adj. Basic Rate (€/hr)	Total Demand (labor-hrs/yr)	Total Cost (€/yr)	FTE/hectare
Operator	27.60	54356.27	€ 1,500,233	0.97
TOTAL			€ 1,500,233	

Consumables

Consumable	Unit Cost (€)	Demand (per yr)	Total Cost (€/yr)	Cost (%)
Omega green algae	7200	item 160.00	€ 1,152,000	55.34
Vibro I - UF membrane	540	m2 381.13	€ 205,810	15.25
Vibro-I membrane	540	m2 735.03	€ 396,916	29.41
TOTAL	-	--	€ 1,754,726	100.00

Utilities

Power Type	Unit Cost	Demand (per yr)	Total Cost (€/yr)	Cost (%)
Std Power	0.10 €/kW-h	2903878.27	€ 278,772.31	100.00
TOTAL			€ 278,772.31	100.00

Fixed Capital Estimate summary

3A. Total Plant Direct Cost (TPDC) (physical cost)		
1. Equipment Purchase Cost		€ 9,208,000
2. Installation		€ 2,026,000
3. Process Piping		€ 2,302,000
4. Instrumentation		€ 2,762,000
5. Insulation		
6. Electrical		
7. Buildings		€ 2,302,000
8. Yard Improvement		
9. Auxiliary Facilities		€ 2,762,000
TPDC		€ 22,374,000

3B. Total Plant Indirect Cost (TPIC)		
10. Engineering		€ 2,237,000
11. Construction		€ 4,475,000
TPIC		€ 6,712,000

3C. Total Plant Cost (TPC = TPDC+TPIC)		
TPC		€ 29,086,000

3D. Contractor's Fee & Contingency (CFC)		
12. Contractor's Fee		€ 1,454,000
13. Contingency		€ 2,909,000
CFC		€ 4,363,000

3E. Direct Fixed Capital Cost (DFC = TPC+CFC)		
DFC		€ 33,449,000

Equipment purchase costs

Quantity/St	Equipment	Unit Costs	Total costs
160/0	Bioreactor ALG-P1	€ 9,000	€ 1,444,000
	Container Volume = 460,00 m3		
36/11	VIBRO-1 MF-101	€ 56,000	€ 2,632,000
	Membrane Area = 60,00 m2		
56/39	VIBRO-2 MF-102	€ 30,000	€ 2,850,000
	Membrane Area = 20,00 m2		
4/0	Storage tank V-101	€ 111,000	€ 444,000
	Vessel Volume = 122,84 m3		
	Unlisted equipment		€ 1,842,000
	Equipment purchase costs		€ 9,212,000

B Appendix B: Algae Refinery S1 economic evaluation

Annual Operating Cost S1

Operating Costs	Annual Cost(€)	%
Downstream		
Raw Materials	€ 1,000	0.04%
Labor-Dependent	€ 823,000	36.05%
Facility-Dependent	€ 567,000	24.84%
Laboratory/QC/QA	€ 62,000	2.72%
Consumables	€ 59,000	2.58%
Waste	€ 14,000	0.61%
Utilities	€ 757,000	33.16%
TOTAL	€ 2,283,000	

Material Cost

Bulk Material	Unit Cost (€)	Annual Amount	Annual Cost (€)	%
HCl (1 M)	0.35	2314 kg	€ 810	96%
NaOH (1 M)	0.36	82 kg	€ 30	4%
TOTAL			€ 839	

Labor Cost

Labor Type	Adj. Basic Rate (€/hr)	Total Demand (labor-hrs/yr)	Total Cost (€/yr)	FTE/ hectare
Operator	27.60		0 € -	0.00
TOTAL			€ 1,500,233	

Consumables

Consumable	Unit Cost (€)	Demand (per yr)	Total Cost (€/yr)	Cost (%)
Vibro I - UF membrane	540	m2 110.00	€ 59,400	100
TOTAL	-	- -	€ 59,400	100

Utilities

Power Type	Unit Cost	Demand (per yr)	Total Cost (€/yr)	Cost (%)
Chilled Water	0.40 €/MT	559826	€ 223,930.50	30%
Steam	12.00 €/MT	6239	€ 74,862.61	10%
Std Power	0.10 €/kW-h	4769007	€ 457,824.64	61%
TOTAL			€ 756,617.75	

Fixed Capital Estimate Scenario 1

3A. Total Plant Direct Cost (TPDC) (physical cost)		
1. Equipment Purchase Cost	€	1,873,000
2. Installation	€	524,000
3. Process Piping	€	468,000
4. Instrumentation	€	562,000
5. Insulation	€	19,000
6. Electrical	€	94,000
7. Buildings	€	468,000
8. Yard Improvement	€	94,000
9. Auxiliary Facilities	€	562,000
TDPC		€ 4,662,000.00
3B. Total Plant Indirect Cost (TPIC)		
10. Engineering	€	466,000
11. Construction	€	932,000
TPIC		€ 1,399,000.00
3C. Total Plant Cost (TPC = TPDC+TPIC)		
TPC		€ 6,060,000.00
3D. Contractor's Fee & Contingency (CFC)		
12. Contractor's Fee	€	303,000
13. Contingency	€	606,000
CFC		€ 909,000.00
3E. Direct Fixed Capital Cost (DFC = TPC+CFC)		
DFC		€ 6,969,000.00

Equipment purchase costs

Quantity/Standby	Equipment	Unit Costs	Total costs
2/0	Homogenizer Rated Throughput = 17,46 m ³ /h	€ 105,000	€ 210,000
1/0	DS-1 Disk-Stack Centrifuge Throughput = 6299,60 L/h	€ 130,000	€ 130,000
1/0	SDR-2 Spray Dryer Dryer Volume = 5135,25 L	€ 172,000	€ 172,000
1/0	SDR-1 Spray Dryer Dryer Volume = 3179,02 L	€ 150,000	€ 150,000
2/1	UF-1 Microfilter Membrane Area = 20,00 m ²	€ 30,000	€ 90,000
3/2	DS-2 Disk-Stack Centrifuge Throughput = 2,03 m ³ /h	€ 107,000	€ 535,000
1/0	R-2 Stirred Reactor Vessel Volume = 12,51 m ³	€ 104,000	€ 104,000
1/0	R-1 Stirred Reactor Vessel Volume = 12,96 m ³	€ 107,000	€ 107,000
	Unlisted Equipment		€ 375,000
	Equipment purchase costs		€ 1,873,000

C Appendix C: Algae Refinery S2 economic evaluation

Annual Operating Cost Refinery S2

Operating Costs	Annual Cost(€) %	
	Downstream	
Raw Materials	€ 1,000	0.04%
Labor-Depende	€ 1,108,000	46.11%
Facility-Depende	€ 382,000	15.90%
Laboratory/QC/C	€ 83,000	3.45%
Consumables	€ 37,000	1.54%
Waste	€ 15,000	0.62%
Utilities	€ 777,000	32.33%
TOTAL	€ 2,403,000	

Material Cost

Bulk Material	Unit Cost (€)	Annual Amount	Annual Cost (€)	%
HCl (1 M)	0.35	2,344 kg	€ 820	96%
NaOH (1 M)	0.36	84 kg	€ 30	4%
TOTAL			€ 851	

Labor Cost

Labor Type	Adj. Basic Rate (€/hr)	Total Demand (labor-hrs/yr)	Total Cost (€/yr)	FTE/ hectare
Operator	27.60	40,151.00	€ 1,108,168	0.72
TOTAL			€ 1,108,168	

Consumables

Consumable	Unit Cost (€)	Demand (per yr)	Total Cost (€/yr)	Cost (%)
Vibro I - UF membrane	540	m2 68.75	€ 37,132	100
TOTAL	-	- -	€ 37,132	100

Utilities

Power Type	Unit Cost	Demand (per yr)	Total Cost (€/yr)	Cost (%)
Chilled Water	0.40 €/MT	571298	€ 228,519.15	98%
Steam	12.00 €/MT	6239	€ 74,869.97	32%
Std Power	0.10 €/kW-h	4,933,184.28	€ 473,585.69	204%
TOTAL			€ 776,974.82	

Annual Operating Cost Drying

Operating Costs	Annual Cost(€) %	
	Downstream	
Raw Materials	€ 1,238	0.12%
Labor-Depender	€ 232,282	22%
Facility-Depende	€ 392,000	37%
Laboratory/QC/Q	€ 17,000	2%
Consumables	€ 367,608	35%
Utilities	€ 42,586	4%
Miscellaneous	€ -	0%
TOTAL	€ 1,052,714	

Material Cost

Bulk Material	Unit Cost (€)	Annual Amount	Annual Cost (€)	%
Water	0.70	1768 m3(STP)	€ 1,238	100%
TOTAL			€ 1,238	

Labor Cost

Labor Type	Adj. Basic Rate (€/hr)	Total Demand (labor-hrs/yr)	Total Cost (€/yr)
Operator	27.60	8416	€ 232,282
TOTAL			€ 232,282

Consumables

Consumable	Unit Cost (€)	Demand (per yr)	Total Cost (€/yr)	Cost (%)
Vibro I - UF membrane	540	m2 680.63	€ 367,608	100
TOTAL	-	- -	€ 367,608	100

Utilities

Power Type	Unit Cost	Demand (per yr)	Total Cost (€/yr)	Cost (%)
Chilled Water	0.40 €/MT	12408	€ 4,963.31	12%
Steam	12.00 €/MT	2408	€ 28,898.22	68%
Std Power	0.10 €/kW-h	90882	€ 8,724.67	20%
TOTAL			€ 42,586.20	

Fixed Capital Estimate S2

3A. Total Plant Direct Cost (TPDC) (physical cost)	
1. Equipment Purchase Cost	€ 1,178,000
2. Installation	€ 329,000
3. Process Piping	€ 294,000
4. Instrumentation	€ 353,000
5. Insulation	€ 12,000
6. Electrical	€ 59,000
7. Buildings	€ 294,000
8. Yard Improvement	€ 59,000
9. Auxiliary Facilities	€ 353,000
TDPC	€ 2,931,000.00
3B. Total Plant Indirect Cost (TPIC)	
10. Engineering	€ 293,000
11. Construction	€ 586,000
TPIC	€ 879,000.00
3C. Total Plant Cost (TPC = TPDC+TPIC)	
TPC	€ 3,811,000.00
3D. Contractor's Fee & Contingency (CFC)	
12. Contractor's Fee	€ 191,000
13. Contingency	€ 381,000
CFC	€ 572,000.00
ma	
DFC	€ 4,382,000.00

Equipment purchase costs

Quantity/Standby	Equipment	Unit Costs	Total costs
1/0	Homogenizer Rated Throughput = 17,46 m3/h	€ 96,000	€ 96,000
1/0	DS-1 Disk-Stack Centrifuge Throughput = 6299,60 L/h	€ 124,000	€ 124,000
1/0	SDR-2 Spray Dryer Dryer Volume = 5135,25 L	€ 146,000	€ 146,000
1/0	SDR-1 Spray Dryer Dryer Volume = 3179,02 L	€ 127,000	€ 127,000
1/0	UF-1 Microfilter Membrane Area = 20,00 m2	€ 34,000	€ 34,000
2/0	DS-2 Disk-Stack Centrifuge Throughput = 2,03 m3/h	€ 109,000	€ 218,000
1/0	R-2 Stirred Reactor Vessel Volume = 12,51 m3	€ 97,000	€ 97,000
1/0	R-1 Stirred Reactor Vessel Volume = 12,96 m3	€ 100,000	€ 100,000
	Unlisted Equipment 375,000		€ 236,000
Equipment purchase costs			€ 1,178,000

Fixed Capital Estimate Dryer

3A. Total Plant Direct Cost (TPDC) (physical cost)	
1. Equipment Purchase Cost	€ 1,150,000
2. Installation	€ 446,000
3. Process Piping	€ 288,000
4. Instrumentation	€ 345,000
5. Insulation	€ 12,000
6. Electrical	€ 58,000
7. Buildings	€ 288,000
8. Yard Improvement	€ 58,000
9. Auxiliary Facilities	€ 345,000
TDPC	€ 2,988,000.00
3B. Total Plant Indirect Cost (TPIC)	
10. Engineering	€ 299,000
11. Construction	€ 598,000
TPIC	€ 896,000.00
3C. Total Plant Cost (TPC = TPDC+TPIC)	
TPC	€ 3,884,000.00
3D. Contractor's Fee & Contingency (CFC)	
12. Contractor's Fee	€ 194,000
13. Contingency	€ 388,000
CFC	€ 583,000.00
3E. Direct Fixed Capital Cost (DFC = TPC+CFC)	
DFC	€ 4,466,000.00

Equipment purchase costs

Quantity/Standby	Equipment	Unit Costs	Total costs
9/7	UF-2 Microfilter Membrane Area = 27,50 m2	€ 36,000	€ 576,000
1/0	SDR-3 Spray Dryer Dryer Volume = 16889,71 L	€ 178,000	€ 178,000
1/0	SL-1 Silo Vessel Volume = 520,94 m3	€ 166,000	€ 166,000
	Unlisted Equipment 375,000		€ 230,000
Equipment purchase costs			€ 1,150,000

D Appendix D: Solar drying techniques

In potential, solar drying is an environmentally friendly, low energy requiring drying technique. However, solar energy has not been widely commercialized due to expensive investments, the variation in intensity and duration of radiation, the needed low skilled manpower, and the required maintenance on equipment [86]. Since almost no literature concerning the drying of algae with solar dryers is available, new developments in solar drying of agricultural crops are reviewed in this section. Solar dryers which are used to dry crops with similar MC (w.b.) as algal paste (above 70%) using suitable temperatures (50-70 °C) are specifically of interest. The variety of the dried crops, the drying conditions, drying methods, and reported figures make it nearly impossible to create a direct comparison between these techniques, limiting the overview to a description of general trends. The large variety of solar dryers are available, varying in size and types, as depicted in Figure 6.

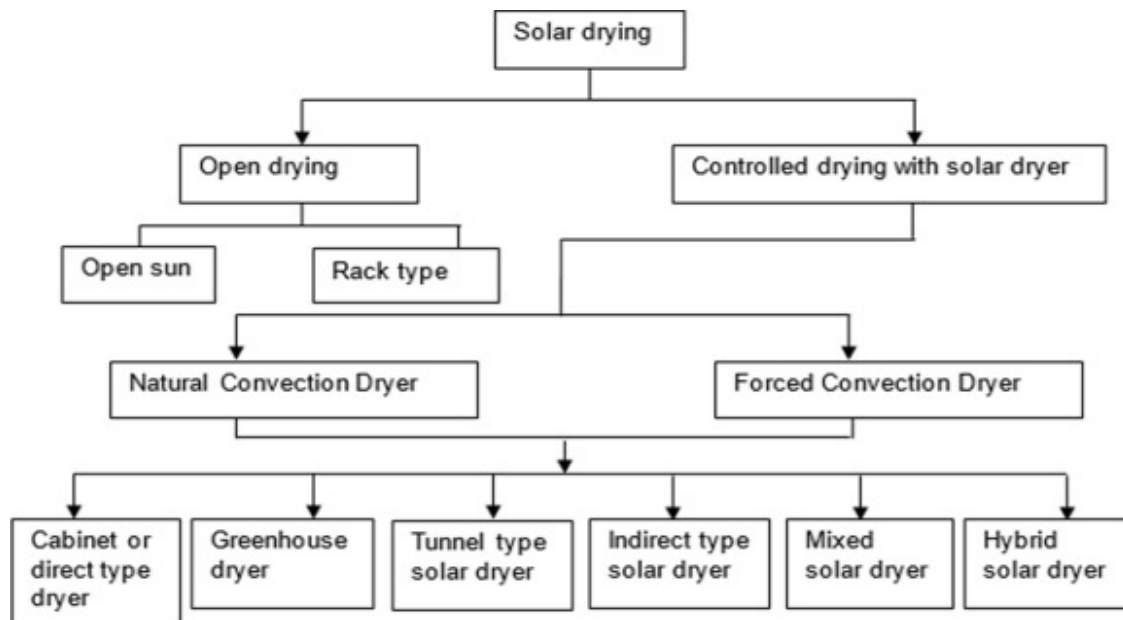


Fig. 6: Classification of solar drying systems, adopted from Lingayat et al.[86]

From the solar drying techniques depicted in Figure 6, open drying system will not be evaluated. The contact of the to be dried material with the open air results in a system which can easily be contaminated by dust, pollutions, bird droppings, insect infestations, degradation through direct solar radiation, and additional loss due to non-uniform and insufficient drying, leading to infestations by fungi, bacteria and other microorganisms. [86, 87].

Natural convection dryers depend on the thermo-syphon effect as the driving force for air circulation during drying. Factors influencing the thermo-syphon effect are solar radiation, air temperature, wind conditions and the collector design [88]. With forced convection dryers, a fan is installed which ensures air circulation, resulting in increased control over the drying rate [89].

Cabinet type dryers and direct type dryers are composed of a transparent cover, such as glass or polycarbonate, through which the solar radiation is transmitted toward the food products [90]. Convective losses need to be limited in order to obtain temperatures suitable for drying. Direct type dryers are able to limit outside contamination, result in better quality products compared to open system drying, and are cheap and easy to fabricate. Downsides are lower drying rates compared to indirect drying configurations when vapor moisture is improperly removed, lower capacity compared

to other configurations, and a reduction of glass cover transmissivity when moisture condensation occurs [86, 90].

Indirect Type Solar Dryers (ITSD) consist of a solar air collector in which the air is heated, after which the heated air is transported towards a drying cabinet in which the to be dried material is placed. This method has the advantage of increased color retention since the product is not exposed to UV radiation, has greater efficiency compared to direct solar drying, and does not result in heat damage due to drying rate control [86]. Many different designs and configurations of the solar air collectors have been studied, such as multiple passes, partial air re-circulation, and the incorporation of heat storage [91, 92, 93, 94]. These different configurations have different benefits. The introduction of a double pass has shown to increase the drying efficiency with 5% compared to a single pass ITSD during drying of red seaweed [91]. With red chillies, a 10% drying efficiency increase was obtained compared to cabinet dryers [92]. The addition of granite rocks on the top layer of the drying cabinet to hold sensible heat in the drying process of Roselle has resulted in a drying time reduction of 21 hours [94].

Hybrid type solar dryers use solar collectors in combinations with auxiliary heaters to increase the operation window and to obtain suitable drying temperatures when solar radiation is insufficient. Auxiliary heaters can be combined with any type of solar dryer, where ITSD types are most commonly used [94, 95]. These types of solar dryers have been used to investigate the usage of solar drying in central Europe, where an ITSD equipped with an electrical water heater, partial air re-circulation, and reflective plate is used to dry banana and tomato slices [96, 97]. This dryer configuration was capable of reaching temperatures of 30-40°C above ambient temperature during summer, suitable temperatures for drying of whole algae [96]. This configuration outperformed open drying significantly, reaching MC (w.b.) of 18% in the same time period where open drying resulted in 62%. However, it shows the limitations of solar drying in areas where solar radiation is limited, such as the desired location for Omega Green in the Netherlands. Another hybrid recirculating design resulted in a energy saving of 70 % in the drying of onion slices at 60 and 70°C [93]. The addition of a LPG burner to a ITSD has resulted in an increase in drying efficiency of 47%, drying tomato slices in 15 hours with an initial MC (w.b.) of 94 % [95].

Tab. 17: Overview developments solar drying studies of high moisture content agricultural crops

Material	Type	MC (w.b.%)		Duration (h)	T (°C)	Ref
		initial	final			
Tomato	ITSD	93	11	11	50	[98]
Red seaweed	Double Pass ITSD	90	10	-	-	[91]
Red Chilli	Double Pass ITSD	90	10	32	52	[92]
Roselle	Double Pass LH ITSD	85	9	14	57	[94]
Onion slices	Partial Recirculation Hybrid ITSD	86	7	-	75	[93]
Tomato	Hybrid ITSD	94	-	15	50	[95]
Banana	Hybrid ITSD	82	18	8	40-50	[96]

Solar drying techniques have been shown to be ineffective for year-round use in areas with similar solar conditions as the Netherlands, only proven effective during the summer period even with hybrid drying techniques [96, 97]. Furthermore, the required low skilled manpower would be a major obstacle in Western-Europe. Some automated systems have been developed, such as the patented hybrid direct type drier of Ecoduna, an Austrian based algae producer [99]. The invention

claims to be able to dry algal paste with an initial concentration between 100 and 200 g/L towards a MC (w.b.) of 20-25 % within 20 minutes by thin layer drying on a moving belt [99]. However, no information is available on the effectiveness, energy consumption, and whether the invention is actually used commercially.

Nonetheless, the developments of drying techniques might be useful for the Moroccan plant of Omega Green, where an ITSD system is already in use. The drying efficiency improvements with the incorporation of re-circulation, multiple passes, heat storage and auxiliary heating could result in an increased operating window for solar drying at the Moroccan Omega Green plant, where the effectiveness of the current solar dryers significantly decreases after the summer period [91, 93, 96].